LEVEL II

AD A074137

COLUMBIA UNIVERSITY
HUDSON LABORATORIES
Contract Nonr-266(84)

ON THE GROWTH OF THE SPECTRUM OF A WIND GENERATED SEA ACCORDING TO A MODIFIED MILES-PHILLIPS MECHANISM AND ITS APPLICATION TO WAVE FORECASTING

by

Tokujiro Inoue

DDC
RECEIVED
SEP 19 1979
C

DDC FILE COPY

This document has been approved for public release and sale; its distribution is unlimited.

New York University
School of Engineering and Science
University Heights, New York, N.Y. 10453

Geophysical Sciences Laboratory TR-67-5

Research Division

July 1967

Best
Available
Copy

UNCLASSIFIED

SECURITY CLASSIFICATION OF THIS PAGE (When Data Entered)

REPORT DOCUMENTATION PAGE		READ INSTRUCTIONS BEFORE COMPLETING FORM
1. REPORT NUMBER	2. GOVT ACCESSION NO.	3. RECIPIENT'S CATALOG NUMBER
4. TITLE (and Subtitle) ON THE GROWTH OF THE SPECTRUM OF A WIND GENERATED SEA ACCORDING TO A MODIFIED MILES-PHILLIPS MECHANISM AND ITS APPLICATION TO WAVE FORECASTING		5. TYPE OF REPORT & PERIOD COVERED 6. PERFORMING ORG. REPORT NUMBER
7. AUTHOR(s) Inoue, Tokujiro		8. CONTRACT OR GRANT NUMBER(s) ~~Nonr-266(84)~~
9. PERFORMING ORGANIZATION NAME AND ADDRESS New York University School of Engineering and Science University Heights, New York, NY 10453		10. PROGRAM ELEMENT, PROJECT, TASK AREA & WORK UNIT NUMBERS
11. CONTROLLING OFFICE NAME AND ADDRESS Office of Naval Research, Code 220 800 North Quincy St. Arlington, VA 22217		12. REPORT DATE JUL 1967 13. NUMBER OF PAGES
14. MONITORING AGENCY NAME & ADDRESS(if different from Controlling Office)		15. SECURITY CLASS. (of this report) UNCLAS 15a. DECLASSIFICATION/DOWNGRADING SCHEDULE

16. DISTRIBUTION STATEMENT (of this Report)

Approved for public release; distribution unlimited.

17. DISTRIBUTION STATEMENT (of the abstract entered in Block 20, if different from Report)

18. SUPPLEMENTARY NOTES

19. KEY WORDS (Continue on reverse side if necessary and identify by block number)

20. ABSTRACT (Continue on reverse side if necessary and identify by block number)

DD FORM 1 JAN 73 1473 EDITION OF 1 NOV 65 IS OBSOLETE

UNCLASSIFIED

COLUMBIA UNIVERSITY
HUDSON LABORATORIES
CONTRACT Nonr-266(84)

New York University
School of Engineering and Science
Department of Meteorology and Oceanography

Geophysical Sciences Laboratory TR-67-5

ON THE GROWTH OF THE SPECTRUM OF A WIND GENERATED SEA ACCORDING TO A MODIFIED MILES-PHILLIPS MECHANISM AND ITS APPLICATION TO WAVE FORECASTING

GSL-TR-67-5

by

Tokujiro Inoue

DDC
RECEIVED
SEP 19 1979
C

83 p.

July 1967

Prepared for
U.S. Naval Oceanographic Office
under
Contract No. N62306-1589, Task Order 3

This document has been approved for public release and sale; its distribution is unlimited.

Table of Contents

Accession for
NTIS GRA&I
DDC TAB
Unannounced
Justification
By
Distribution/
Availability Codes
Dist | Avail and/or Special
A

List of Figures

List of Figures (cont.)

Acknowledgments

The author sincerely wishes to thank Professor Willard J. Pierson, Jr. for his guidance and encouragement. Without his help, it would have been very difficult to carry out this study. The author also wishes to thank Professors Gerhard Neumann, Leo J. Tick, and A. D. Kirwan for their suggestions and advice, and Mr. Vincent Cardone for valuable discussions of meteorological problems. Dr. T.P. Barnett provided advance copies of his doctoral dissertation and of his measurements, with Mr. Wilkerson, of the growth of waves off the east coast. This material provided valuable data for this study. Professor O.M. Phillips sent Xerox copies of the page proofs of his new text. The opportunity to study the turbulent stress contribution to the exponential growth rate at an early stage of the analysis is appreciated. Thanks are also extended to Miss Ming-Shun Chang, and Messrs. Hong Chin and Leslie W. Longaker for their help.

This research was sponsored by the United States Naval Oceanographic Office under Contract N62306-1589, Task Order No. 3. The continued help of Mr. Marvin Burkhart in the administration of this work and in locating data sources is greatly appreciated.

Abstract

It is necessary to develop detailed numerical forecasting techniques that accurately specify the process of wave generation because the need for accurate wave forecasts is increasing. The growth of the wave spectrum can be approximated by the combined effect of two mechanisms to a point where the crest of the wave breaks on a nonlinear effect becomes dominant.

One mechanism is the Phillips resonance mechanism for wave generation, and the other is the exponential growth mechanism, originally proposed by Miles. Recently, this second growth mechanism was revised by Phillips in terms of the wave-induced atmospheric perturbations. Calculations suggest that this new mechanism explains the available observations, which had previously been unexplainable from the original instability growth mechanism.

To verify the theory, various spectra estimated from wave observations are used, along with measurements provided by fetch limited field experiments made by Snyder and Cox. After some assumptions about energy dissipation are applied, the spectral-growth equation, which is a function of frequency, wind speed, and duration (or fetch), is obtained.

The partially developed sea-spectral shapes provided by the spectral growth equation for several different wind speeds are shown and compared to previous work. The proposed spectral growth shows faster development in an early growing stage (or

short fetch), and slower growth in the last stages. It takes from 35 to 40 hours or 700 to 1000 nautical miles to reach a fully developed sea for a 40 knot wind. The growth rate of the significant wave height is about the same as the results of Sverdrup and Munk.

The proposed expression for the spectral growth is applied in a numerical forecasting computer program to the North Atlantic for the month of December 1959. The time history of the hindcasted significant wave height and the spectral density for low frequencies are compared to the British weather ships' observed data. The wave height shows good agreement with the observed, with the bias calculated to be less than +2 feet and the RMS error less than 5 feet. Excellent verification is also obtained with Argus Island data.

short fetch), and slower growth in the last stages. It takes from 35 to 40 hours or 700 to 1000 nautical miles to reach a fully developed sea for a 40 knot wind. The growth rate of the significant wave height is about the same as the results of Sverdrup and Munk.

The proposed expression for the spectral growth is applied in a numerical forecasting computer program to the North Atlantic for the month of December 1959. The time history of the hindcasted significant wave height and the spectral density for low frequencies are compared to the British weather ships' observed data. The wave height shows good agreement with the observed, with the bias calculated to be less than +2 feet and the RMS error less than 5 feet. Excellent verification is also obtained with Argus Island data.

1. Introduction

In the modern high-speed computer era of today, the techniques for forecasting ocean waves are being studied not only for their purely scientific content but also for the vast wealth of information that can be supplied to such practical problems as shipping, ship designing, and forecasting natural disasters. The past several years have shown an ever-increasing interest in all phases of oceanographic activity. This, then, necessitates a greater understanding of the natural phenomena called oceanic surface waves. Consequently, the study and forecasting of ocean waves must not be limited to only one ocean, but to all three of the world oceans. The use of large, high-speed computers has made rapid and precise determinations of oceanic wave characteristics feasible.

The actual study of ocean wave forecasting can be said to have begun during World War II by Sverdrup and Munk (1947). This study introduced the concepts of significant wave height, H, wave duration, t, fetch, F, steepness (wave height/wave length) δ, and wave age (wave phase speed/wind speed) β, as well as relationships between non-dimensional quantities such as gF/u^2, gt/u, δ and β (where g = gravitational acceleration, and u = wind speed). If either gF/u^2 or gt/u were determined, then δ and β can be found. δ and β were then used to determine the wave height H, and the wave speed C. Several years later, Bretschneider revised this method.

In 1952, the successful application of wave spectra concepts to ocean waves was accomplished in studies of randomness of the sea

surface (Pierson and Marks, 1952). This allowed the idea of a composite ocean wave consisting of different frequencies and amplitudes to be incorporated into a forecasting scheme. Prior to this, the classical method of studying ocean waves considered each wave to be a sinusoid. Also about this time, Longuet-Higgins (1952) made a statistical study of ocean wave properties and presented statistical relationships for the significant wave height, the average height of the one-tenth highest waves and the mean wave height in terms of the variance of a wave record. In the following years, Neumann (1953) proposed a spectral form and co-cumulative spectra (CCS-curves) that were derived from data taken visually on board a ship and off Long Branch, New Jersey.

By incorporating these ideas, Pierson, Neumann and James (1955) were able to develop a new wave forecasting technique based on spectral concepts. This new forecasting technique was very different from the significant height-significant period method in that a great amount of information could be gained about the nature of ocean waves.

Thus in the middle 1950's, two schools of thought existed for the "technique" of forecasting ocean waves--the "significant height" school and the "spectral" school.

With the improvement of wave recording instrumentation (i.e., Tucker, 1956), more accurate observations became available. These data analyses were then followed by many proposals of the growth and spectral form of ocean waves (i.e., Darbyshire, 1955, 1959; Bretschneider, 1959). Several attempts were made to measure the directional spectrum. Coté et al (1960), for instance, worked with

data obtained from pairs of aerial stereophotographs while Longuet-Higgins et al (1963) dealt with data obtained from a buoy. But most of the studies were directed towards finding the form of the one-dimensional spectrum. With the host of proposals, came many differences of opinion. For instance, Darbyshire concluded that the significant wave height was proportional to the square of the wind speed whereas Neumann (1953) concluded that the proportionality was to the 2.5th power. These discrepancies were discussed at the Conference on Ocean Wave Spectra (Ocean Wave Spectra, 1963). A study of these discrepancies was made by Pierson (1964) in terms of the variation of wind speed with height. The use of a wind profile to normalize the wind speeds to the same height resulted in a better agreement among the proposed relations between significant wave height and wind speed.

While a wave is growing due to wind effects, the high frequency range of the spectrum grows more rapidly than the low frequency band because of greater energy input. At the same time, dissipation caused by wave-wave interaction, breaking waves, and viscous effects is also increasing and thus a so-called "equilibrium range" of the spectrum is rapidly approached. Phillips (1958) found the general character of this equilibrium range and proposed an expression of the form $\alpha g^2/\omega^5$ (where α = constant, g = gravitational acceleration, and ω = angular frequency) for the spectrum in this range. Pierson and Moskowitz (1964) then proposed a spectral form for a fully developed sea that was based on the similarity theory of Kitaigorodskii (1961) and data taken by British weather ships.

The development of high-speed electronic computers allowed the field of ocean wave forecasting to make significant advances. Large-scale numerical wave forecasting techniques were attempted (Baer, 1962). The generation and growth processes of waves which were not understood to any appreciable extent at this time were incorporated by use of energy growth tables. It was assumed that the transient spectrum had the same shape as the fully developed sea spectrum for lower wind speeds that produced the same significant wave heights. Up until this time, forecasting was done manually by first employing the various graphs.

The demand for better prediction accuracy led to the study of wave generation, growth and the partially developed sea spectrum. The study of wave generation and growth dates back to the Helmholtz instability theory (Lamb, 1932). This Kelvin-Helmholtz model could not adequately explain wave growth since it required stronger winds than are actually observed to generate waves.

Jeffreys (1925), in his studies on the initial phases of wave formation, introduced the concept of a sheltering coefficient. This was an expression for the increase of pressure on the windward side and decrease of pressure on the leeward side when wind passed over a pre-existent wave. The pressure difference distribution was then used to determine a number called the sheltering coefficient empirically. Experiments on a solid wavy model later showed Jeffreys' results to be about an order of magnitude too large. Sverdrup and Munk (1947) suggested that a smaller value could be obtained, and they took into account the tangential stress acting on

the sea surface in addition to the normal stress. This, however, leads to a contradiction since a tangential stress causes waves to be rotational and actual observations have shown waves to be almost irrotational.

It should be noted that the sheltering coefficient concept assumes pre-existent waves. If the sea surface were calm with no wavy motions, then waves could not grow.

A coupling mechanism between turbulent components of the atmosphere and sea for wave generation from a glassy, calm sea was later proposed by Phillips (1957). This, in essence, said that a resonance between the air-sea system could occur when a component of the surface pressure distribution moved at the same speed as a free surface wave of the same wave number. This resonance would then cause waves to be generated even from calm sea surface conditions.

In another attempt to overcome the sheltering coefficient difficulties, Miles (1957) put forth another theory after computing the amplitude and lag of the pressure fluctuations over waves in terms of properties of the logarithmic wind profile. This theory said that the mean rate of energy transferred from the parallel shear flow to the surface wave is proportional to the curvature of the wind profile, and inversely proportional to the slope of the wind profile at the height where the mean wind velocity is the same as the phase speed of the wave component under investigation.

In further work in this field, Miles (1959) obtained a solution to the Orr-Sommerfeld equation after including the effects of a viscous term. A combined resonance-instability model for wave

generation was also worked out by Miles (1960). Lighthill (1962) later gave a physical interpretation to this model.

Snyder and Cox (1966) made a series of field experiments (based on these new generation theories) to study the growth of a wave component in a limited fetch area. Their results confirmed the effects of the two proposed mechanisms although a difference in the magnitude of the growth rate was found.

With the existence of these two new theories, the study of wave forecasting can now be carried out from a new point of view, namely that of wave generation. An attempt to employ these two theories in terms of spectral concepts has already been made (Inoue, 1966). Large-scale forecasting schemes are also attempting to incorporate these ideas (Pierson, Tick, and Baer, 1966).

Thus, more precise and detailed forecasting of deep water ocean waves can now be accomplished by utilizing wave generation concepts. The purpose of this study, therefore, is to predict the character and spectrum of deep water ocean waves at a given location and time by use of a computer-based technique utilizing the concepts of wave generation mentioned above.

2. Generation and growth of the waves

In order to forecast ocean waves, a study must be made to determine how spectra of the waves can grow. When a component of the spectrum is considered, that spectral component can be expressed in the linear form in the early stage, for nonlinear effects at this stage may be neglected.

$$\frac{d}{dt} S(f, t, \vec{x}) = A(f, u(t, \vec{x})) + B(f, u(t, \vec{x}))\, S(f, t, \vec{x}) \qquad (2.1)$$

where $S(f, t, \vec{x})$ is the spectral density and $A(f, u(t, \vec{x}))$ and $B(f, u(t, \vec{x}))$ are unknown quantities to be determined. If these two functions, A and B, are known, the growth of the spectra can be computed for an early growing stage. In the old model (Inoue, 1966), these two quantities were estimated as

$$A(u) = 1.4 \times 10^{-8} u^3$$

$$B(f, u) = 6.27(u/c)^2 e^{-0.017(c/u)^4} f \qquad (2.2)$$

where u is the wind speed (knots) at 19.5 m anemometer height and c is the phase speed of the component f. The A term was just approximated, and it must be a function of frequency. The B term is also changed in terms of the new theory.

The pressure fluctuations on the sea surface can be decomposed into two categories. One represents the contribution of the atmospheric turbulent eddies and the other is the contribution induced by the air flow over the sea surface. The sea surface can be expressed by the form, $d\zeta(\vec{k})\, e^{i\vec{k}\cdot(\vec{x} - \vec{c}\,t)}$, where $\vec{k}$ is a wave number and $d\zeta(\vec{k})$ is a random complex quantity. The air over that sea surface induces a pressure distribution given by $d\hat{w}(\vec{k}, t)\, e^{i\vec{k}\cdot(\vec{x} - \vec{c}\,t)}$. If the phase of $d\hat{w}(\vec{k}, t)$ is the invariant with respect to $d\zeta(\vec{k})$, the mean

$\langle d\hat{w} \rangle$ is a pressure field induced by a sea whose wave number k is the same.

The relation between the pressure distribution and the sea surface wave amplitude was shown (Miles, 1957, 1959) in the idealized form:

$$p = \mathrm{Re}\{(a + ib)\,\rho_a u_1^2 k\zeta\} \tag{2.3}$$

where a and b are real, non-dimensional quantities depending on the wind profile, ρ_a is the density of air, u_1 is u_*/k_o (u_* is the friction velocity and k_o is von Karman's constant), and ζ is the sea surface.

Phillips used a more realistic description which is expressed by a random wave amplitude $d\zeta(\vec{k})$ and an induced random pressure $d\hat{w}(\vec{k}, t)$.

$$\langle d\hat{w} \rangle = (\nu + i\mu)\,\rho_w c^2 k d\zeta(\vec{k}) \tag{2.4}$$

where ν and μ are non-dimensional coupling coefficients, ρ_w is the water density, c is the phase speed, and the notation, $\langle\ \rangle$, represents an averaging over time in a frame of reference moving in the direction $\vec{k}$ at the appropriate phase speed.

Thus the pressure field is a combination of two parts: one is induced from the sea configuration which is expressed as above; and the other is a random quantity that comes from the atmospheric turbulence. This turbulent pressure supplies energy over a wide frequency region, and an induced pressure caused by the sea surface configuration feeds back to the sea and also contributes to the growth of the wave.

Phillips (1966) solved the equation governing the growth of a

wind generated sea under the assumption that the water is irrotational and that a linealized free surface boundary condition could be used. The surface displacement spectrum $\Psi(\vec{k}, t)$ was obtained. When time t is larger than an integral time scale, and $\omega t >> 1$, $\Psi(\vec{k}, t)$ is expressed by using the wave number, frequency atmospheric pressure spectrum $\Pi(\vec{k}, \omega)$ as

$$\Psi(\vec{k}, t) = \frac{\pi \Pi(\vec{k}, \omega)}{\rho_w^2 c^2} \left(\frac{\sinh \mu \omega t}{\mu \omega} \right) \tag{2.5}$$

Miles (1960) also obtained this relationship. If $\mu\omega t$ is much less than one, then $\sinh \mu\omega t \rightarrow \mu \omega t$ so that (2.5) becomes

$$\Psi(\vec{k}, t) = \frac{\pi \Pi(\vec{k}, \omega)}{\rho_w^2 c^2} t \tag{2.6}$$

Equation (2.6) shows that the wave spectrum grows linearly with time, t, and the atmospheric turbulent fluctuation spectrum. This atmospheric turbulence spectrum shows its maximum at the frequency $\omega = \vec{k} \cdot \vec{u}_c$, where $\vec{u}_c$ is the convection velocity. Therefore the sea surface spectral component becomes dominant at the frequency. f, which is the same frequency as the maximum turbulent spectral component. This is a typical resonance phenomenon.

If $\mu\omega t$ is much larger than one, then $\sinh \mu\omega t \rightarrow e^{\mu\omega t}/2$, so that equation (2.5) can be simplified to

$$\Psi(\vec{k}, t) = \frac{\pi \Pi(\vec{k}, \omega)}{2\rho_w^2 c^2 \mu\omega} e^{\mu\omega t} \tag{2.7}$$

This equation (2.7) shows that the wave spectrum grows exponentially

with time t in the growing stage $\mu\omega t >> 1$, and this is an instability growth mechanism.

Thus, there are two different stages in the generating and growing sea spectrum. First the sea starts to grow from the glassy, calm sea in terms of the resonance mechanism, and then, later the growth by an instability mechanism is involved. The latter mechanism dominates the former, and the sea grows exponentially. Jeffreys tried to determine the atmospheric pressure distribution induced by this wave motion empirically by introducing a sheltering coefficient concept.

These mechanisms can be interpreted in equation (2.1) as follows. First the sea is calm, and there is no spectral energy over the entire frequency range, and no contribution is made by the second term BS. Then the sea grows, and the second term plays an important role. In equation (2.1), the first term is caused by the atmospheric turbulent pressure fluctuation, and the second term is due to the instability mechanism. This is also evident when equation (2.7) is differentiated with respect to time t. Then,

$$\frac{d}{dt}\Psi(\vec{k}, t) = \Psi(\vec{k}, t)\,\mu\omega \tag{2.8}$$

This is exactly the same expression as (2.1) if the first term A on the right hand side is negligibly small.

3. Resonance mechanism growth; the A term

The atmospheric turbulent fluctuation spectrum is needed to get the surface displacement spectrum $\Psi(\vec{k}, t)$. Although this study is concerned with one-dimensional spectra, it will start with the three-dimensional pressure spectrum, because the data used were obtained

with a narrow band sensor. Let $p(x, y, t)$ be the pressure at the point (x, y) at time t; then the correlation function $R(\xi, \eta, \tau)$ is

$$R(\xi, \eta, \tau) = \langle p(x, y, t)\ p(x+\xi,\ y+\eta,\ t+\tau) \rangle \tag{3.1}$$

where ξ and η are deviations from x and y along their axes, and τ is a time lag. Then the pressure spectrum can be shown to be

$$\Pi(\vec{k},\omega) = \frac{1}{(2\pi)^3} \int_{-\infty}^{\infty} d\ \vec{\xi}\ d\tau\ R(\vec{\xi}, \tau) \cos(\vec{k} \cdot \vec{\xi} - \omega\tau) \tag{3.2}$$

where $\vec{\xi}$ is the vector form for ξ and η.

Priestly (1966) made a field measurement of the longitudinal, lateral and diagonal correlation of the atmospheric pressure over grass, and this result is used.

The space-time covariance $R(\xi, \eta, \tau)$ is transformed in a Fourier manner, and the spectral density is

$$K(\xi, \eta, \omega) = \frac{1}{2\pi} \int_{-\infty}^{\infty} R(\xi, \eta, \tau)\, e^{-i\omega\tau}\ d\tau \tag{3.3}$$

Priestly assumed that the spectral density can be expressed as

$$K(\xi, \eta, \omega) \simeq \phi(\omega)\, e^{-\gamma|\xi| - \delta|\eta| - i\varkappa\xi}$$

where $\phi(\omega)$, γ, and δ are determined from the experiment, and $\varkappa = \omega/u_c$. u_c is a convection velocity. Then equation (3.2) becomes

$$\Pi(\vec{k},\omega) = \mathrm{Re}\left\{\frac{1}{(2\pi)^2}\int_{-\infty}^{\infty} d^2\vec{\xi}\,[\phi(\omega)\,e^{-\gamma|\xi|-\delta|\eta|}]\,e^{i(\vec{k}\cdot\vec{\xi}-\varkappa\xi)}\right\} \tag{3.4}$$

Then

$$\Pi(\vec{k},\omega) = \mathrm{Re}\left\{\frac{\phi(\omega)}{(2\pi)^2}\int_{-\infty}^{\infty} d\xi\, e^{|\xi|[-\gamma+i(k_x-\varkappa)]}\int_{-\infty}^{\infty} d\eta\, e^{|\eta|[-\delta+i(k_y)]}\right\}$$

where k_x and k_y are wave numbers of the x and y components. This can be expressed in the following form:

$$\Pi(k,\omega) = \frac{4\phi(\omega)}{(2\pi)^2}\left[\frac{\gamma}{\gamma^2+(k\cos\theta-\varkappa)^2}\right]\left[\frac{\delta}{\delta^2+k^2\sin^2\theta}\right] \tag{3.5}$$

where k is defined as $\omega^2 = gk$ and θ is an angle from the wind direction.

According to Priestly's experiment, γ and δ were determined as

$$\begin{aligned}\gamma &= 0.33\varkappa^{1.28}\\ \delta &= 0.52\varkappa^{0.95}\end{aligned} \tag{3.6}$$

Priestly's observation shows some tendency for γ to be constant for $\varkappa < 0.02\,(m^{-1})$, but in this study γ is treated as a function of $\varkappa$ as defined in equation (3.6).

$\phi(\omega)$ was found to be expressed as

$$\phi(\omega) = \Phi\psi(\omega) \tag{3.7}$$

where Φ is a scaling factor and $\psi(\omega)$ is determined from Priestly's measurement, and

$$\psi(\omega) \simeq \frac{1.23}{\omega^2} \tag{3.8}$$

In order to determine the scaling factor Φ, the field experiment data obtained by Snyder and Cox (1966) were used, and Φ was assumed to be proportional to the fourth power of the wind speed,

$\Phi \propto \text{const} \cdot u^4$.

The one-dimensional spectrum is then obtained by integrating (3.5) with respect to the angle θ from $-\pi/2$ to $\pi/2$, and the A term is written in the form

$$A(f, u) = \frac{2\pi k \omega^3}{\rho_w g^2} \int_{-\pi/2}^{\pi/2} \Pi(\vec{k}, \omega)\, d\theta \tag{3.9}$$

After putting all the constants together as A^*, equation (3.9) becomes

$$A(f,u) = \int_{-\pi/2}^{\pi/2} \frac{A^*(\omega)^{5.25}\, u^{2.25}}{[\frac{1}{4}(\frac{\omega}{u})^2 + (k \sin\theta)^2][\frac{1}{9}(\frac{\omega}{u})^{2.5} + (k \cos\theta - \frac{\omega}{u})^2]}\, d\theta \tag{3.10}$$

where $\omega = 2\pi f$, u is the wind speed at a certain anemometer height, $k = \omega^2/g$, and A^* will be determined later from observational data.

4. Instability mechanism growth; the BS term

Miles (1957, 1959) studied this instability type growth in terms of inviscid laminar flow. Phillips (1966) took into account the undulatory turbulent flow due to the waves. This atmospheric perturbation due to the sea is quite different from the other mechanisms and affects the wave growth factor μ strongly. The Phillips theory is summarized as an important part of this study in this section.

The wind velocity in a moving frame with speed $\vec{c}$ is expressed by

$$\vec{u} = \vec{U}(z) + \vec{u'}(x, y, z, t) + \vec{U}_p(x, z) - \vec{c} \tag{4.1}$$

for a y-direction averaged wave surface $\langle \zeta \rangle = a \cos kx$, where

$\vec{U}(z)$ is the mean wind velocity, $\vec{u'}(x, y, z, t)$ is a random fluctuation from the mean, and $\vec{U}_p(x, z)$ is a perturbation induced by the sea configuration.

Following the derivations of Phillips, assume the atmosphere to be an incompressible fluid; then the stream function ψ is defined as

$$\begin{aligned} \partial\psi/\partial z &= U\cos\theta + U_p - c \\ \partial\psi/\partial x &= -W_p \end{aligned} \tag{4.2}$$

Because U_p and W_p are periodic along the x-coordinate, the stream line of the mean motion is

$$\psi = \int_{z_m}^{z} \{U(\zeta)\cos\theta - c\}\, d\zeta + \psi(z)\, e^{ikx} = \text{const.} \tag{4.3}$$

where z_m is the height of the matched layer which is $U(z_m)\cos\theta = c$.

Then investigate how the momentum flux shifts from the atmosphere to the wave. Use the equations of motion and average over the y-direction. The mean stress balance, then, is obtained by taking the complete average on the derived equation. That is,

$$\frac{\partial}{\partial x_j}\overline{U_{p_i} U_{p_j}} + \frac{\partial}{\partial x_j}\overline{u_i' u_j'} = -\frac{1}{\rho}\frac{\partial \bar{P}}{\partial x_i} + \nu\frac{\partial^2 U_i}{\partial x_j^2} \tag{4.4}$$

If the fluid is non-viscous, the component of this equation in the x-direction is

$$\frac{\partial}{\partial z}\left\{\overline{U_p W_p} + \overline{u'w'}\right\} = 0 \tag{4.5}$$

The first term represents the wave-induced stress and the second term represents the Reynolds turbulent stress, and the total stress

is the sum of the wave-induced stress, τ_w, and the turbulent stress, τ_t. Only the first term remains in inviscid laminar flow. However, Phillips showed that this is also a sufficient approximation even if the flow is turbulent.

Then, considering the wave induced Reynolds stress by using the product ΩW_p, where Ω is the vorticity of the wave-induced perturbation and W_p is the vertical component of the induced perturbation,

$$\Omega W_p = (\frac{\partial}{\partial z} U_p - \frac{\partial}{\partial x} W_p) W_p = \frac{\partial}{\partial z} (U_p W_p) + \frac{1}{2} \frac{\partial}{\partial x} (U_p^2 - W_p^2) \tag{4.6}$$

which is derived under the assumption of incompressibility, $\partial U_p/\partial x = -\partial W_p/\partial z$.

Integrate (4.6) with respect to z, and take an x-average. Then

$$\rho \int_z^\infty \overline{\Omega W_p} \, dz = -\rho \overline{U_p W_p} = \tau_w(z) \tag{4.7}$$

If $z = 0$, equation (4.7) becomes

$$\tau_w(0) = \rho \int_0^\infty \overline{\Omega W_p} \, dz \tag{4.8}$$

The variations in the mean vorticity are supposed to be proportional to the mean vorticity gradient and the magnitude of the undulations

$$|\Omega| \propto |U''(z) \, \delta \cos\theta| \tag{4.9}$$

because the basic flow has a mean vorticitv distribution $U'(z)\cos\theta$. The quantity, δ, is the displacement of the mean streamline about

the average height, z, and is derived from equation (4.3).

Outside the matched layer, δ_o is expressed by

$$\delta_o = \frac{W(z_1)}{k[U(z_1)\cos\theta - c]} \tag{4.10}$$

Therefore,

$$\overline{\Omega W_p} = M\left\{\frac{-U''(z)\,\overline{W_p^2}(z)\cos\theta}{U(z)\cos\theta - c}\right\} \tag{4.11}$$

In an inviscid, laminar flow, variations in Ω and W_p are exactly out of phase, so that this term must be zero. However, Phillips considered that there is no reason to suppose Ω and W_p to be uncorrelated in turbulent flow. So this term cannot be neglected while we neglect it in a laminar flow model. Thus, outside the matched layer, equation (4.10) survives and M is determined as $M \simeq 1.6 \times 10^{-2}$.

Inside the matched layer, the displacement of the mean stream lines δ_m is expressed by

$$\delta_m = \left\{\frac{4W_p(z_m)}{kU'(z_m)\cos\theta}\right\}^{1/2} \tag{4.12}$$

The increment to the wave-induced Reynolds stress, τ_{wm}, across the matched layer is derived from

$$\tau_{mw} = M_m \rho \left\{\frac{-U''}{kU'}\overline{W_p^2}\right\}_{z=z_m} \tag{4.13}$$

According to Miles' quasi-laminar analysis, $M_m = \pi$ in the above equation. This is the form originally proposed by Miles (1957).

Therefore, the total wave-induced Reynolds stress is a sum of these two equations in turbulent flow.

$$\tau_w(o) = M_m \rho \left\{ \frac{-U''}{kU'} \overline{W_p^2} \right\}_{z=z_m} + M\rho \left\{ \int_o^\infty \frac{(-U'')\, \overline{W_p^2} \cos\theta}{k|U(z)\cos\theta - c|} dz \right\} \tag{4.14}$$

Two different values are used for outside the matched layer and for inside the matched layer, respectively, as the approximations to W_p as it appears in equation (4.14).

Outside the matched layer:

$$W_p = -iNka\{U(z)\cos\theta - c\} e^{-kz} e^{ikx} \tag{4.15}$$

Inside the matched layer:

$$W_p = -\frac{iNak^3 e^{ikx}}{U'(z_m)\cos\theta} \int_{z_m}^\infty \{U(z)\cos\theta - c\}^2 e^{-kz}\, dz \tag{4.16}$$

where N is a constant and has a different value depending on the layer under consideration, and a is the amplitude of the free surface wave.

By using the coupling parameters given in (2.4), the induced surface pressure distribution can be expressed as $(\nu + i\mu)\rho_w c^2 k a e^{ikx}$. The imaginary part, μ, plays an important role in the growth of the wave, and can be expressed by

$$\mu = \frac{2\tau_w(o)}{\rho_w c^2 k^2 a^2} \tag{4.17}$$

where $\tau_w(o) = \langle p \rangle_\zeta \langle \partial\zeta/\partial x \rangle$, and ζ is the free surface. The

combination of (4.14), (4.15), (4.16), and (4.17) yields

$$\mu = \frac{\rho_a}{\rho_w} \frac{1}{c^2 k} \left\{ \frac{M_m N^2 k^2}{\cos^2\theta} \left(\frac{-U''}{U'^3} \right)_{z=z_m} \left(\int_{z_m}^{\infty} [U\cos\theta - c]^2 e^{-kz}\, dz \right)^2 \right.$$

$$\left. + M \int_0^{\infty} N^2 (-U'') \cos\theta \, |U\cos\theta - c| \, e^{-2kz}\, dz \right\} \qquad (4.18)$$

To relate the curvature U'' and the slope U' of the wind profile to the wind profile, we assume neutral atmospheric stability. So the wind profile becomes logarithmic and is expressed by

$$U(z) - \frac{c}{\cos\theta} = \frac{u_*}{k_o} \ln \frac{z}{z_m} \qquad (4.19)$$

where u_* is the friction velocity, and k_o is a von Karman constant. From equation (4.19), the roughness parameter z_o is expressed by

$$z_o = z_m \exp\left\{ \frac{-k_o c}{u_* \cos\theta} \right\} \qquad (4.20)$$

Phillips used a relationship for z_o suggested by Charnock (1955) to connect the roughness parameter and friction velocity. For aerodynamically rough flows, Charnock's form is

$$z_c \simeq 0.078 \frac{u_*^2}{g} \qquad (4.21)$$

To evaluate equation (4.18), N^2 must be estimated. $N^2 \sim \frac{1}{3}$ for $z > z_m$ and $N^2 = 1$ for $z < z_m$ are used.

The value of the growth rate μ (or $B(f,u)/f$ in (2.1)) is

shown in figure 3 by a dashed line.

Kitaigorodskii and Volkov (1965) gave data and analyses that tended to show that the roughness parameter is not simply a function of the friction velocity, but is also a function of the sea state. If this is correct, the expression for z_o shown above is not appropriate. If this type of expression is allowed, Kitaigorodskii and Volkov gave a different value for the constant as

$$z_o \simeq 0.035 \frac{u_*^2}{g} \tag{4.22}$$

As mentioned above, it is not appropriate to formulate a relationship between the roughness parameter and the friction velocity over the ocean. Their data also scattered widely, but a mean square distribution of $\ln z_o$ fitted very well with the Kolmogorov's test of goodness of fit to a normal distribution in a given u_* interval. If this expression of z_o is used in the first term of (4.18), the curve of the growth rate μ is raised as shown in figure 3.

In the region of $u_*/c > 0.06$, the phase speed is small and the matched layer lies at a high wind profile curvature U'', and the Miles formula, the first term in equation (4.18), gives a large contribution to the waves. When u_*/c decreases, so does the wind profile curvature and that term becomes less dominant. But the second term of (4.18) which is due to the undulatory turbulent flow becomes dominant and the growth rate μ increases again. This is a very interesting phenomenon, and some observational data also show this tendency. The discussion of the observational data is given in the next section.

5. Data and formulation for growth

To verify these growth mechanisms, five different kinds of observations were used. The weather conditions were studied for the period from April 1955 to March 1960, and the spectra for various synoptic situations were estimated from the wave records obtained by the British weather ships, "Weather Explorer" and "Weather Reporter" (Moskowitz, Pierson, and Mehr, 1962, 1963, 1965). These data were taken with the Tucker shipborne wave recorder (Tucker, 1956) at the weather stations A, I, J, and K. The location of the ships are as follows. Station A: 62°N, 33°W; Station I: 59°N, 19°W; Station J: 52.5°N, 20°W; Station K: 45°N, 16°W. Moskowitz et al picked 460 wave records from that period. The wave observations were made at three or six hour intervals, and were approximately fifteen minutes long. The spectra have a frequency range of $0 \sim 0.333$ cycles per second. The wind speed was measured at 19.5 m above sea level.

Wave records obtained at Argus Island were also studied. The data used were taken with a resistance wire wave recorder on Argus Island tower (32°N, 65°W) for the period from 20 November to 30 November 1961 (Pickett, 1962; DeLeonibus, 1962). This tower is located 25 miles southwest from Bermuda Island, and the water is approximately 200 feet deep. The observations were made every three hours and each record was 20 minutes long. The frequency covers $0 \sim 0.266$ cycles per second. The anemometer height was 42.5 m above the sea.

The data obtained on FLIP (Floating Instrument Platform) were also checked. The position of FLIP was approximately

39°20'N, 148°20'E in the North Pacific, and the observations were three hours long and were taken twice a day. Sea surface wave spectra were estimated from the records of two vibrotron transducers at 31 m and 88 m below the sea surface (Snodgrass et al, 1966). The data were spectrally analyzed for six 30-minute pieces from three hours of continuous records for the period of September 1963 (Inoue, 1967).

These three sets of data include fully developed seas, growing seas, and decaying seas. Only the data from the growing sea, however, are useful in this study, and little change of meteorological conditions between two observations is preferable. From this point of view, three criteria were set at first: (1) significant wave height had to increase; (2) the wind speed had to change less than two knots within three hours; (3) the wind direction had to change less than 45° within the three hours between two successive observations. When the data passed these criteria, the spectra were checked again as follows. The spectra that contained dominant spectral components in the low frequency swell, or two or more big peaks were rejected. Under these conditions, only ten pairs of spectra were chosen. Besides these criteria, one more limitation was imposed for the purpose of this study. This is (4), the spectral component of the second observation had to be less than one-third of the spectral component of the fully developed sea for a particular frequency. The amount of available spectral component growth data was then very limited, but these spectra and spectral components seem to be really growing stage spectra.

Fetch limited wind wave studies were made by Snyder and Cox (1966) and by Barnett and Wilkerson (1966). Snyder and Cox made an observation to see how a particular spectral component grew with fetch in the Bahamas in the spring of 1963. Barnett and Wilkerson took observations by using an airborne altimeter on 20 February 1965. The flight was taken along the direction SSW up to 190 nautical miles off the New Jersey coast. These two field experiments were made mainly for the purpose of the investigation of the Miles-Phillips mechanism.

Snyder and Cox towed rafts arranged 17 m apart downwind with a group velocity of waves with a 17 m wavelength, and measured the development of that component wave. The wind speed ranged from about 10 to 20 knots, and the anemometer height was 6.1 m above the sea surface. The data were obtained for a total of 51 hours.

To evaluate the constant A^* in the A term (3.10), the value obtained by Snyder and Cox was used. Their wave recorder had an effective beam width of 20 degrees. By taking this width into account, the final form of their result is expressed by

$$A(f,u) = \int_{-\pi/2}^{\pi/2} \frac{9.84 \times 10^{-15} (\omega)^{5.25} u^{2.25}}{\left[\frac{1}{4}\left(\frac{\omega}{u}\right)^2 + (k \sin\theta)^2\right]^2 \left[\frac{1}{9}\left(\frac{\omega}{u}\right)^{2.5} + (k\cos\theta - \frac{\omega}{u})^2\right]} d\theta \qquad (5.1)$$

where u is a wind speed in m/sec at 19.5 anemometer height. (The wind speed was corrected to this anemometer height from the wind observed at the lower anemometer height). $k = \omega^2/9.8$.

The result of this form is plotted in figure 1 which also has the value of the A term estimated by Snyder and Cox. The one-

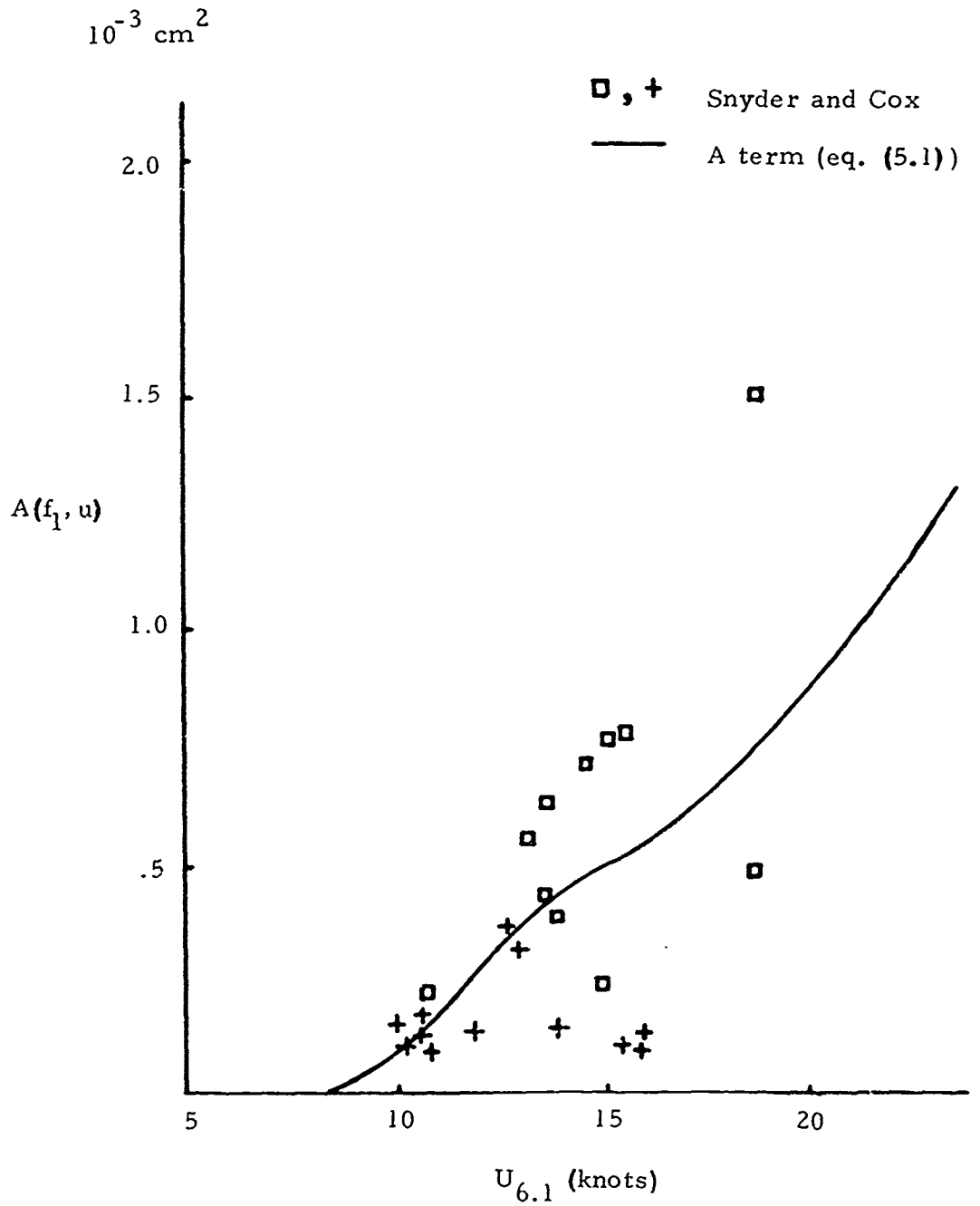

Figure 1

Resonance mechanism growth $A(f_1,u)$ for a 20° directional band width versus wind speed and f_1 = 0.3 cps.

dimensional representation for this form is shown in figure 2 as a function of wind speed in knots. As pointed out in Section 3, γ follows a tendency toward being constant and not a $\kappa^{1.28}$ law for $\kappa < 0.02$ (m^{-1}). Then the forward leading edge of the curve in figure 1 may be smaller and steeper for high wind speeds.

Clearly, from the physical meaning of the resonance mechanism, the sea is excited by an atmospheric turbulent pressure, and the growth of the A term is dominant at the component that has the same velocity as the turbulent convection velocity. The location of the peak on each curve is about at the frequency whose phase velocity is the same as the convection velocity. In the previous study (Inoue, 1966), this A term was simply treated as a function of wind speed over the entire frequency range which was not sufficient.

In order to investigate the growth with respect to an instability mechanism, five different kinds of data were checked as mentioned previously. Unfortunately, few spectra of FLIP for the analyzed period passed the criteria described previously. The reason was that there were mostly moderate seas in September, and when a strong wind was blowing, criteria (2) and (4) were not satisfied.

It is difficult to detect the A term growth from the spectra estimated by the British weather ship data, and the Argus Island tower data. Therefore, the A term was considered to be given by equation (5.1), and this growth quantity was subtracted from the observation to study the BS term growth. If the value of the A term is smaller than the actual spectral component, the BS quantity can be studied by investigating

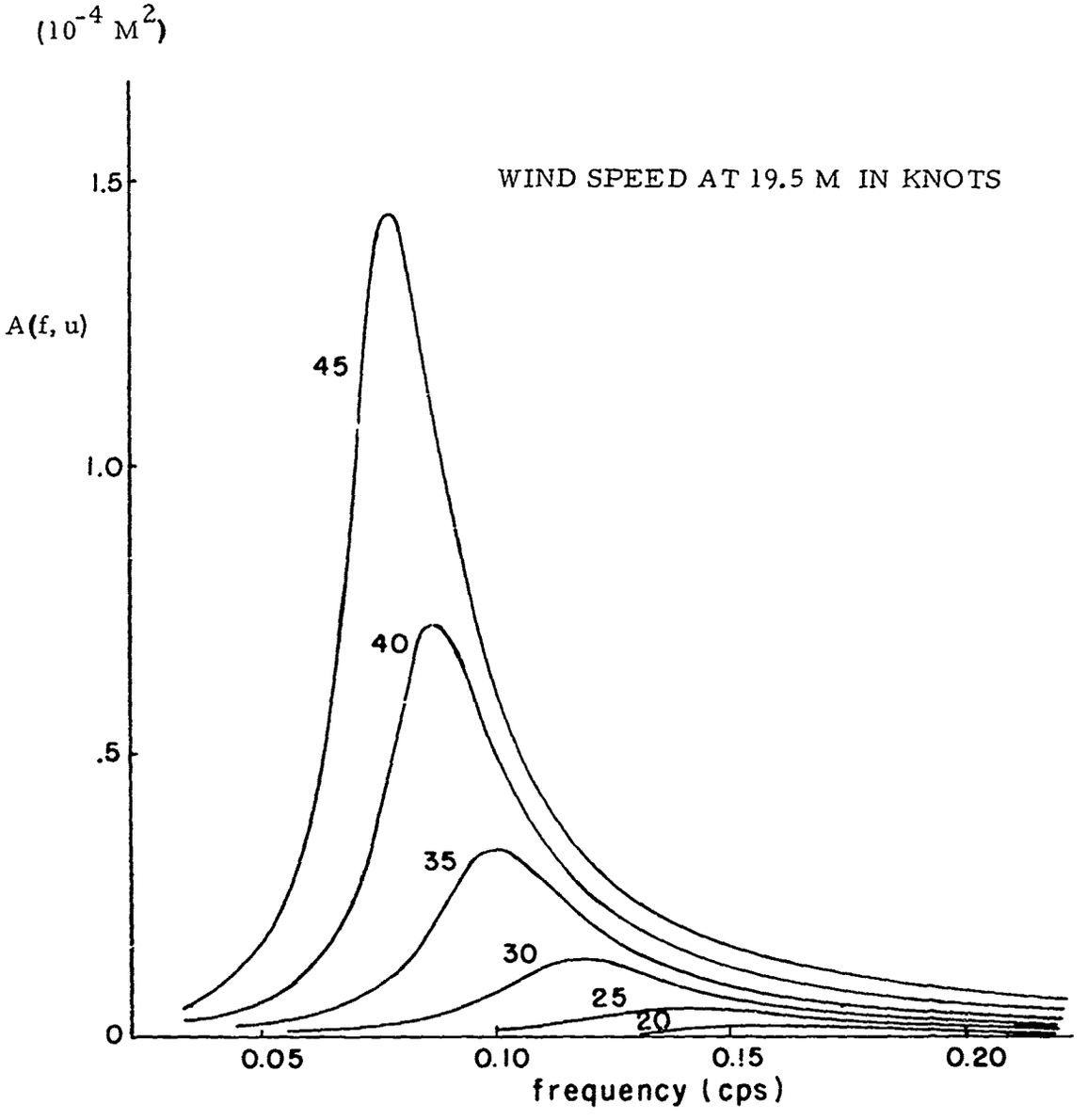

Figure 2

Resonance mechanism growth A(f,u)
for different wind speeds.

$$\left(\ln \frac{S_1}{S_o}\right) \Big/ \Delta t \cdot f \tag{5.2}$$

where S_o is an initial spectrum and S_1 is a spectrum after Δt hours.

In Section 4, the friction velocity u_* was used to evaluate the roughness parameter z_o. In the actual ocean, it is a very difficult problem to determine friction velocity, and sometimes an approximation, $u = 9u_*/k_o$, has been used, where k_o is von Karman's constant.

However, Kitaigorodskii and Volkov (1965) showed that there was a close relationship between the roughness parameter and the sea state. When the roughness parameter is plotted against the wave height, the observed data scatter widely, and there is no strong correlation between two quantities. However, the following form was found by considering that the roughness parameter was dependent on both the average phase speed and the wave height.

$$z_o = 0.120\, \bar{H} \exp\left\{-\frac{k_o \tilde{c}}{u_*}\right\} \tag{5.3}$$

where $\bar{H}$ is an average wave height, and $\tilde{c}$ is an average phase speed of the sea. If the relation of $\bar{H} = 0.625\, \bar{H}_{\frac{1}{3}}$ is introduced where $\bar{H}_{\frac{1}{3}}$ is the significant wave height, then

$$z_o = 0.075\, \bar{H}_{\frac{1}{3}} \exp\left\{-\frac{k_o \tilde{c}}{u_*}\right\} \tag{5.4}$$

When the atmospheric condition is neutral, the wind profile becomes logarithmic. The average wind speed at height z is

expressed by using this roughness parameter.

$$\bar{u}(z) = \frac{u_*}{k_o}\left\{\ln z - \ln\left[0.075\,\bar{H}_{\frac{1}{3}}\exp\left(-\frac{k_o\tilde{c}}{u_*}\right)\right]\right\} \tag{5.5}$$

and

$$u_* = \frac{k_o(\bar{u} - \tilde{c})}{\ln\dfrac{z}{0.075\bar{H}_{\frac{1}{3}}}} \tag{5.6}$$

If the spectrum of that sea state is known, an average phase speed $\tilde{c}$ can be expressed by

$$\tilde{c} = \frac{g\tilde{T}}{2\pi} = \frac{g}{2\pi}\sqrt{\frac{\Sigma S(f)}{\Sigma f^2 S(f)}} \tag{5.7}$$

where $\tilde{T}$ is the average period of the sea.

As the above equation for the friction velocity (5.6) shows, u_* is strongly affected by the average speed $\tilde{c}$. While the waves are growing at a certain wind speed, the spectrum develops from the high frequency region, and then u_* is large because of small $\tilde{c}$. As the sea grows further, $\tilde{c}$ becomes large, and u_* decreases. Physically, this can be interpreted as the fact that the movement of the wave system is approaching the movement of the atmospheric system.

The friction velocities for the data from the British weather ships, Argus Island tower, and the airborne altimeter were computed by using the estimated spectra and equation (5.6) for u_*. The spectra used were modified by applying the $\alpha g^2/\omega^5$ law for the equilibrium range for the high frequency region if the available

spectra did not cover the full frequency range. The experiment of Snyder and Cox (1966) was made on a single component and could not reproduce spectra correctly. Therefore, the friction velocity for that case was estimated from the observed wind speed and the drag coefficient at 10 m, c_{10}, proposed by Deacon and Webb (The Sea, 1962).

The observed results were plotted against u_*/c to study the BS term growth in figure 3. The value on the ordinate shows B/f (or growth factor μ). The data obtained by Snyder and Cox (1966), and Barnett and Wilkerson (1966) are shown by + and · symbols, respectively. The other coded symbols plotted are from the British weather ship data (Moskowitz, Pierson, and Mehr, 1962, 1965, 1965) and Argus Island tower data (Pickett, 1963). Careful attention must be given to the data from the Argus Island tower because the geographical conditions (the distance from both the east coast of the United States and Bermuda, and the water depth) and the small difference between $\bar{u}$ and $\tilde{c}$ might introduce some error. The frequency appears to have been high enough to permit its generation to full development for the fetch and duration possible at Argus Island. The data for these observations such as coded symbol, record number, wind speed, significant wave height, and location are listed in Appendix I.

In figure 3 there is a difference between the observed results shown by the coded symbols and the theoretical value shown by the dashed and dotted lines [both lines are theoretical but different roughness parameters are used] in the range of high

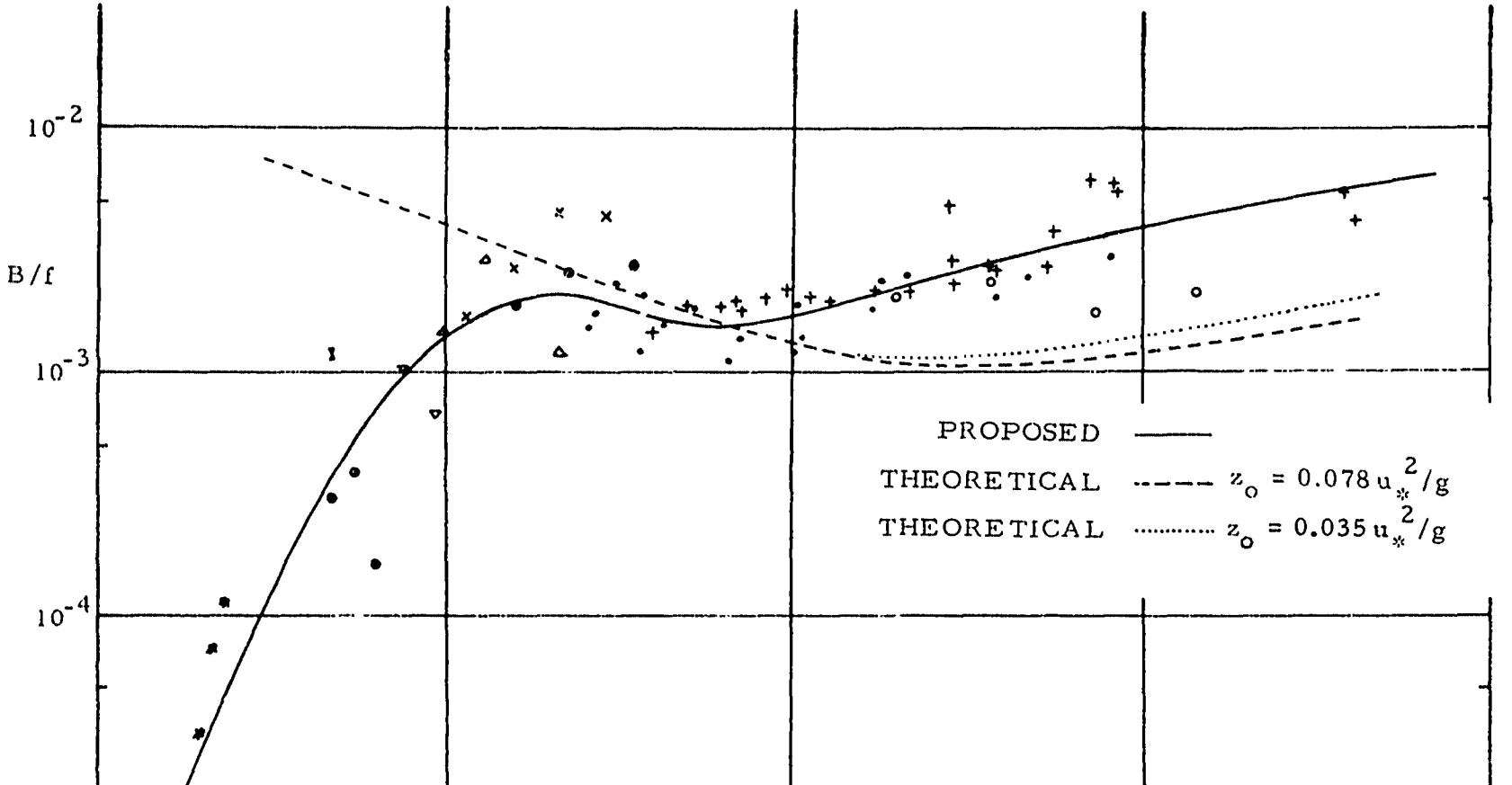

Figure 3 Growth rate of the instability mechanism, $B(f,u_*)/f$, versus u_*/c. (See Appendix I for coded symbols.)

and low u_*/c. In the low u_*/c region, all the observed results decrease as u_*/c decreases, and there is no result close to the theoretical values for $u_*/c < 0.025$. In the range where $u_*/c > 0.06$, the theoretical values are lower than the observed results, and the difference is about a factor of 3. When the roughness parameter (4.22) given by Kitaigorodskii and Volkov (1965) is used, the theoretical value increases, but not by very much. The difference between the theoretical value and the proposed growth factor was estimated as a factor of 8 in previous work (Inoue, 1966).

Shemdin and Hsu (1966) carried out an experiment in a water tank on the atmospheric pressure distribution in the vicinity of progressive water waves. In the experiment, the growth of mechanically generated waves was also studied and compared with the theoretical result (Miles' theory). Some of the experimental results show growths three times greater than the theoretical results, and confirm the observed results shown in figure 3.

The wind profile was treated as a logarithmic profile, but the profile depends on the atmospheric stability, as is well known. Most data used in this study show a slightly negative value for the air-sea temperature difference. The air-sea temperature differences for the British weather ship data are listed in Appendix II. In Snyder and Cox's experiment, the conditions were nearly neutral, and the largest difference was -0.7°C. Because the data of Barnett and Wilkerson were taken from an airplane, the measurement of temperature was not made along the flight track. However, it was reported that the difference was -6°C ~ -10°C on the light ships

stationed near the track.

When the atmosphere is unstable, the friction velocity will be higher to an extent determined by the Richardson number. As mentioned earlier, the observed air-sea temperature difference was slightly negative, and the observed results were plotted for neutral conditions by using equation (5.6). When the air-sea temperature difference is taken into account, the plotted points of the result might be shifted a little toward the right. However, both sets of observations--the British weather ship data and the airborne altimeter data--were taken during a strong wind, and a high wind makes the Richardson number

$$Ri = \frac{g}{\theta} \frac{\partial \theta}{\partial z} \Big/ \left(\frac{\partial u}{\partial z}\right)^2$$

small. Therefore, even though the observed air-sea temperature difference was slightly negative, the growth rate was plotted against the neutral conditions u_* (5.6).

The most important difference in the new instability growth mechanism proposed by Phillips (1966) is that the mechanism is expressed by two terms--one is the term originally proposed by Miles and the other is a term contributed from outside the matched layer due to the undulatory turbulent flow over the waves. The latter mechanism makes the growth rate μ (or B/f) large in the low u_*/c region. However, the observed growth rate does not show any increasing tendency as the proposed theoretical value increases (figure 3).

One of the most dominant results in this study is the "bump" existing in the range of $u_*/c = 0.025 \sim 0.040$ in figure 3. When the growth rate in the old model (Inoue, 1966) was studied, the same kind

of figure was plotted in order to study the Miles mechanism. And the observed growth rate B/f also showed this rise (at that time, the quantity, B/f, was plotted as a function of u/c). This rise and fall toward decreasing u_*/c is not small. It is quite significant because the abscissa has a logarithmic scale. The explanation of why this hillock occurs could not be given before. At first, the method of data selection was thought improper, but the data were picked in the manner of the criteria mentioned in Section 5, and the wind speeds were also nearly constant during the two successive observations. The growth rate by the newly proposed process fits well to the observed data in the range of $u_*/c = 0.03 \sim 0.05$ in figure 3. Thus, this "bump" can be considered to be explained as the result of the undulatory turbulent flow theory proposed by Phillips in that range of u_*/c.

When the friction velocity u_* is constant, the spectral component whose wavelength or phase speed is large falls in the range of small u_*/c. The matched layer of such a wave component is high in the atmosphere, and the effect due to the undulatory turbulent flow of that longer wave may be considered to be small.

In order to apply these wave generation mechanisms, the observed growth rates were used. The curve of the growth factor B/f is obtained from the plotted observed data, and is shown by the solid line in figure 3. The variation of $B(f, u_*)$ is expressed by

$$B(f,u_*) = \left\{0.00139e^{-7000[(u_*/c)-0.031]^2} + 0.725\left(\frac{u_*}{c}\right)^2 e^{-0.0004(c/u_*)^2}\right\} f \quad (5.9)$$

The unit is (sec^{-1}).

As a form for this type of growth, Snyder and Cox (1966) and also Barnett (1967) estimated that it was linear with respect to u/c, and was zero for $u/c < 0.8 \sim 0.9$.

In equation (5.9), the friction velocity formula proposed by Kitaigorodskii and Volkov is used. According to their theory, u_* is a function of the sea state, namely, the average wave height and average wave speed. Therefore the B term growth is also a function of the sea state. Or, stated another way, the input energy for this growth depends on the sea state. When this growth rate is only a function of u/c, the energy input of this mechanism is constant for the same wind speed for a particular frequency. However, if B/f is a function of u_*, the growth rate has different values even for the same wind speed and same frequency. Excluding the "bump" in the range $0.03 \sim 0.05\ u_*/c$, when the seas are low, u_*/c is high, and more energy is fed in, generally speaking. The more the sea grows, and the smaller u_*/c becomes, the less the energy that can be fed in. This is just a general description, and the "bump" must be taken into account. However, this is a behavior different from that of the previous mode'

6. Spectral growth

If a nonlinear effect is not involved in the growing stage, equation (2.1) can be used to find the generation and growth of the wave spectra. As the wave grows, however, nonlinear effects such as breaking waves and wave-wave interactions are introduced.

Ocean wave spectra have been studied during the last decade, and many spectral forms and growth rates were proposed. Known

and unknown properties were also discussed (e.g., Neumann and Pierson, Ocean Wave Spectra, 1963). Among those properties, Phillips (1958) investigated breaking waves by using similarity considerations. As the wind waves grow, the wavy surface becomes unstable at some stage. Then the waves break, lose energy, and keep their stability. There is some region called the "equilibrium range" which attains a statistical equilibrium. In this range, Phillips proposed that the spectral form can be written as

$$S_e(\omega) \propto \alpha g^2/\omega^5 \tag{6.1}$$

The energy transfer between different wave components in a random wave field was also studied by Hasselmann (1962, 1963a, 1963b).

Equation (2.1) is linear, and the spectral component grows to an infinite value with time. But once waves generate, energy dissipation will follow more or less immediately. Dissipation has not been studied very much so far, and little is known about it. There is, however, some general agreement on the spectral growth sequence. The spectral component increases slowly after starting from a zero initial condition, but dissipation is not dominant. The growth is linear in the early stage; then it becomes exponential. This is obvious from the first and second terms in equation (2.1). When this spectral component comes close to the steady state, dissipation also increases, and the growth is slowed down. Finally, that spectral component reaches the fully developed sea spectral value. When the input energy and the dissipated energy balance over the whole frequency range, the sea can be considered to be a fully developed sea. There is some question as to whether or not a

"fully developed sea" exists in the actual ocean, but many observed data confirm that there is a stage that can be said to be a fully developed sea and that the spectral components are proportional to the f^{-5} law in the high frequency region.

When the growth of a spectral component is considered, this energy dissipation might be assumed to be a function of the ratio of the spectrum at a particular moment to the fully developed sea spectrum , and as a good approximation, equation (2. 1) may be expressed by

$$\frac{d}{dt}S(f,t,\vec{x}) = [A(f,u) + B(f,u_*)\,S(f,t,\vec{x})] - [A(f,u) + B(f,u_*)\,S(f,t,\vec{x})]\left[\frac{S(f,t,\vec{x})}{S_\infty(f)}\right]^2 \qquad (6.2)$$

where $S_\infty(f)$ is a fully developed sea spectrum for that wind speed. In equation (6.2), the first term represents the energy input from the atmosphere to the waves in terms of a resonance mechanism and an instability mechanism, and the second term includes only dissipation quantities and represents the energy loss. The fully developed sea spectrum form proposed by Pierson and Moskowitz (1964) is used.

This fully developed sea spectrum form is given as

$$S_\infty(\omega) = \frac{\alpha g^2}{\omega^5}\, e^{-\beta(\omega_o/\omega)^4} \qquad (6.3)$$

where $\alpha = 8.10 \times 10^{-3}$, $\beta = 0.74$, and $\omega_o = g/u$.

In order to make the manipulation of (6.2) easier, another function is introduced in the A term. This change does not affect the growth very much. Then (6.2) is changed to the form

$$\frac{d}{dt} S(f,t,\vec{x}) = \left[A\left\{ 1 - \left(\frac{S}{S_\infty}\right)^2 \right\}^{1/2} + BS \right]\left[1 - \left(\frac{S}{S_\infty}\right)^2 \right] \tag{6.4}$$

The solution to this equation for a zero initial spectrum condition and an infinite fetch is

$$S(f,t) = \frac{A\{\exp(Bt) - 1\}}{B}\left[1 + \left\{ \frac{A(\exp(Bt) - 1)}{BS_\infty} \right\}^2 \right]^{-1/2} \tag{6.5}$$

where A and B are represented in equations (5.1) and (5.9) respectively. If t is in hours, then A and B are expressed by the following form to give a spectrum in $(m^2 sec)$.

$$A(f,u) = \int_{-\pi/2}^{\pi/2} \frac{3.54 \times 10^{-11} (\omega)^{5.25}\, u^{2.25}}{\left[\frac{1}{4}\left(\frac{\omega}{u}\right)^2 + (k\sin\theta)^2\right]\left[\frac{1}{9}\left(\frac{\omega}{u}\right)^{2.5} + \left(k\cos\theta - \frac{\omega}{u}\right)^2\right]} d\theta \tag{6.6}$$

$$B(f,u_*) = \left[5e^{-7000[(u_*/c) - 0.031]^2} + 2612\left(\frac{u_*}{c}\right)^2 e^{-0.0004(c/u_*)^2} \right] f \tag{6.7}$$

If the sea is not calm initially, equation (6.8) may be used.

$$S(f,t) = \frac{A[\exp\{B(t+t_o)\} - 1]}{B}\left[1 + \left\{ \frac{A \exp\{B(t+t_o) - 1\}}{BS_\infty} \right\}^2 \right]^{-1/2} \tag{6.8}$$

where

$$t_o = \frac{1}{B} \ln\left[1 + \frac{BS_o}{A\{1 - (S_o/S_\infty)^2\}^{1/2}} \right]$$

and S_o is an initial spectral component.

The spectral growth was computed for wind speeds of 20, 25, 30, 35, 40, and 45 knots by using (6.5). The results are shown in

figures 4(a) through (f) as a function of wind duration for infinite fetch.

If the wind has been blowing for a long time, the sea is then independent of time, and equation (2.1) becomes

$$\frac{d}{dt} S(f, x) = c_g \frac{\partial}{\partial x} S(f, x) = A(f, u) + B(f, u_*) S(f, x) \tag{6.9}$$

From $x = c_g t$, the spectral growth as a function of fetch was also computed for constant wind speeds, and the results are shown in figures 5(a) through (f).

The initial condition of the sea was zero for spectral growths both as functions of fetch and duration. From this initial condition, the friction velocity, u_*, cannot be obtained from equation (5.6). Therefore, the initial friction velocity u_* is approximated. The spectrum for the first time step is computed, and then u_* for the following time step is computed from the values of $\tilde{c}$ and $\bar{H}_{\frac{1}{3}}$ obtained from the spectrum for the first time step.

As the waves grow, the quantity $(\bar{u} - \tilde{c})$ influences the friction velocity more and more. That is, the spectra grow in the low frequency band, and $\tilde{c}$ approaches the wind speed $\bar{u}$. According to equation (5.6), u_* decreases as $(\bar{u} - \tilde{c})$ becomes small. Therefore, the friction velocity has a tendency to decrease as the waves grow. When we consider the following form,

$$u_* = \sqrt{c_{10}}\, u$$

where c_{10} is a drag coefficient at 10 m above the sea surface. c_{10} also decreases as the waves grow. Kitaigorodskii and Volkov's

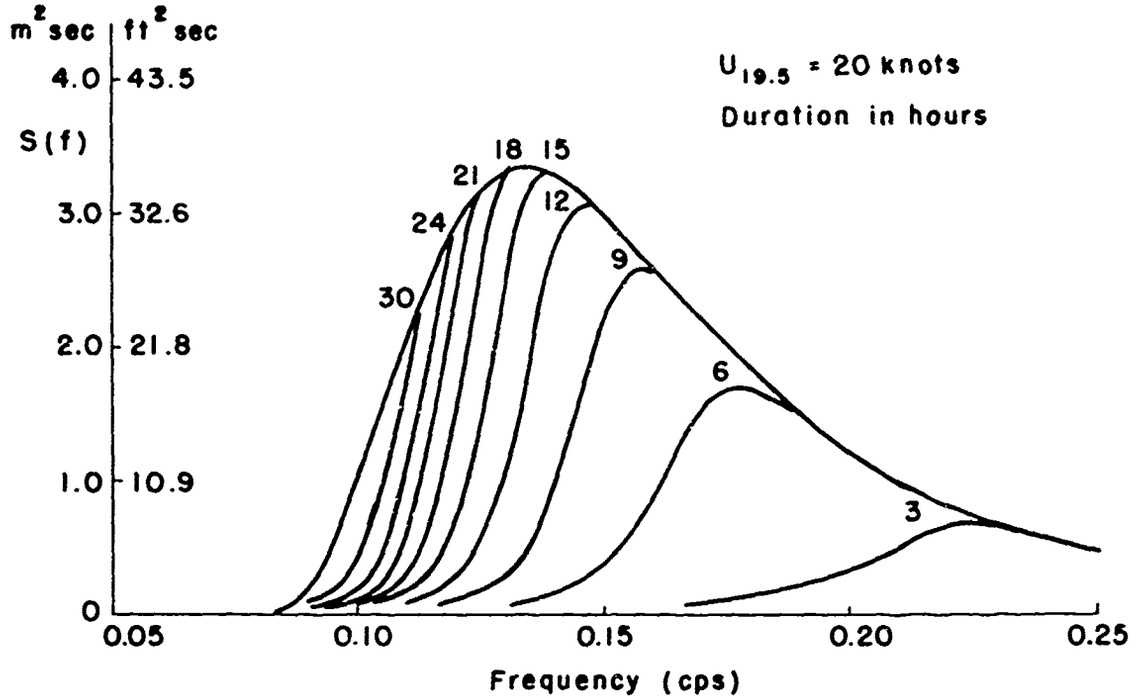

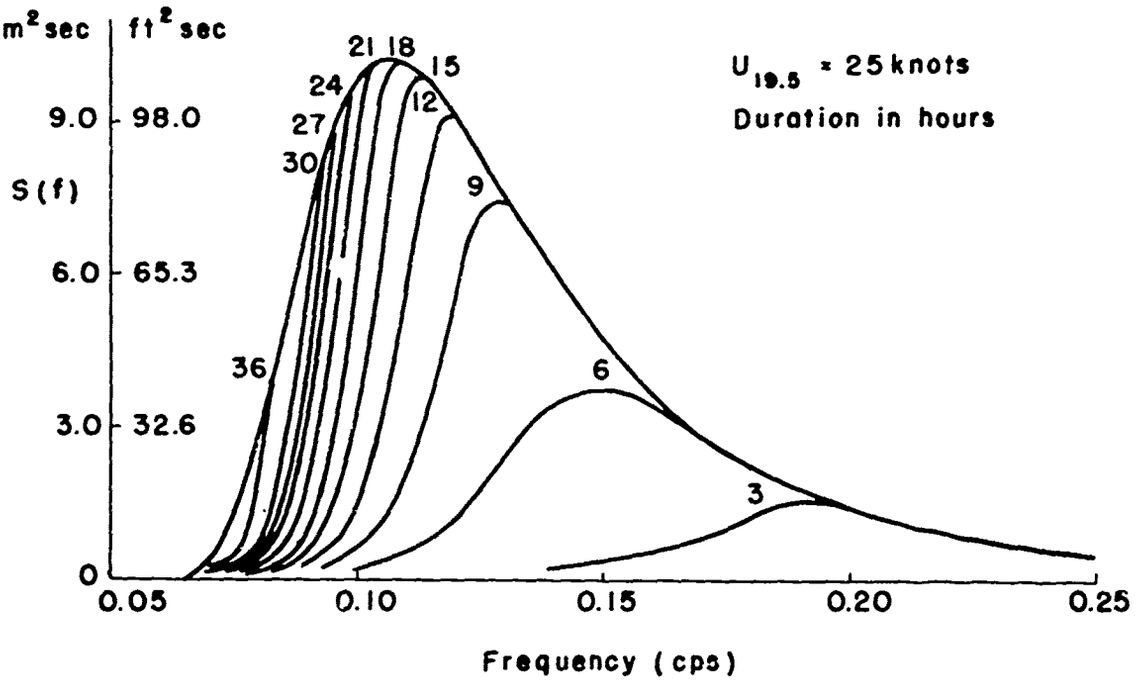

Figures 4a and 4b Growth of the spectrum for 20 and 25 knot winds with duration in hours.

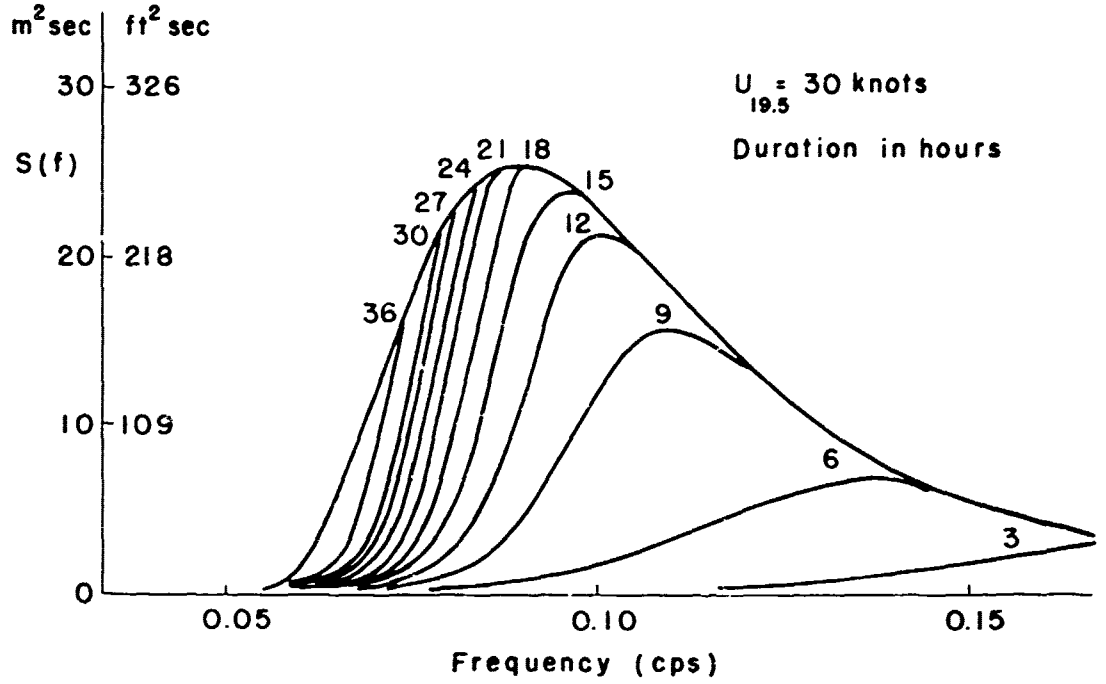

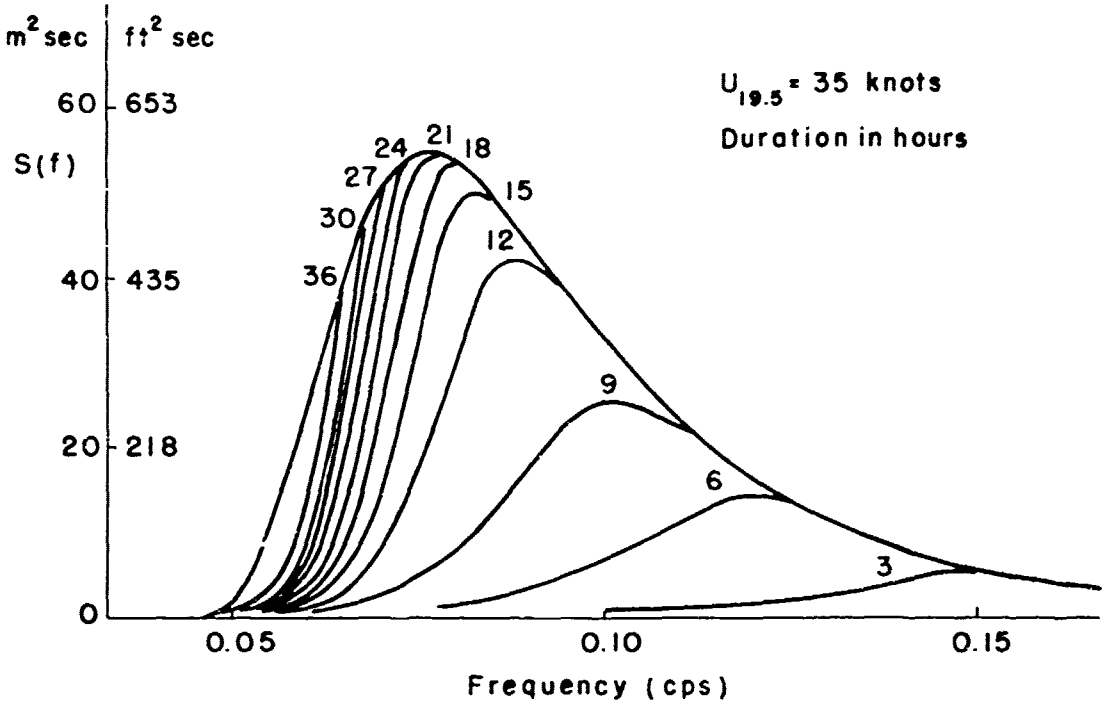

Figures 4c and 4d Growth of the spectrum for 30 and 35 knot winds with duration in hours.

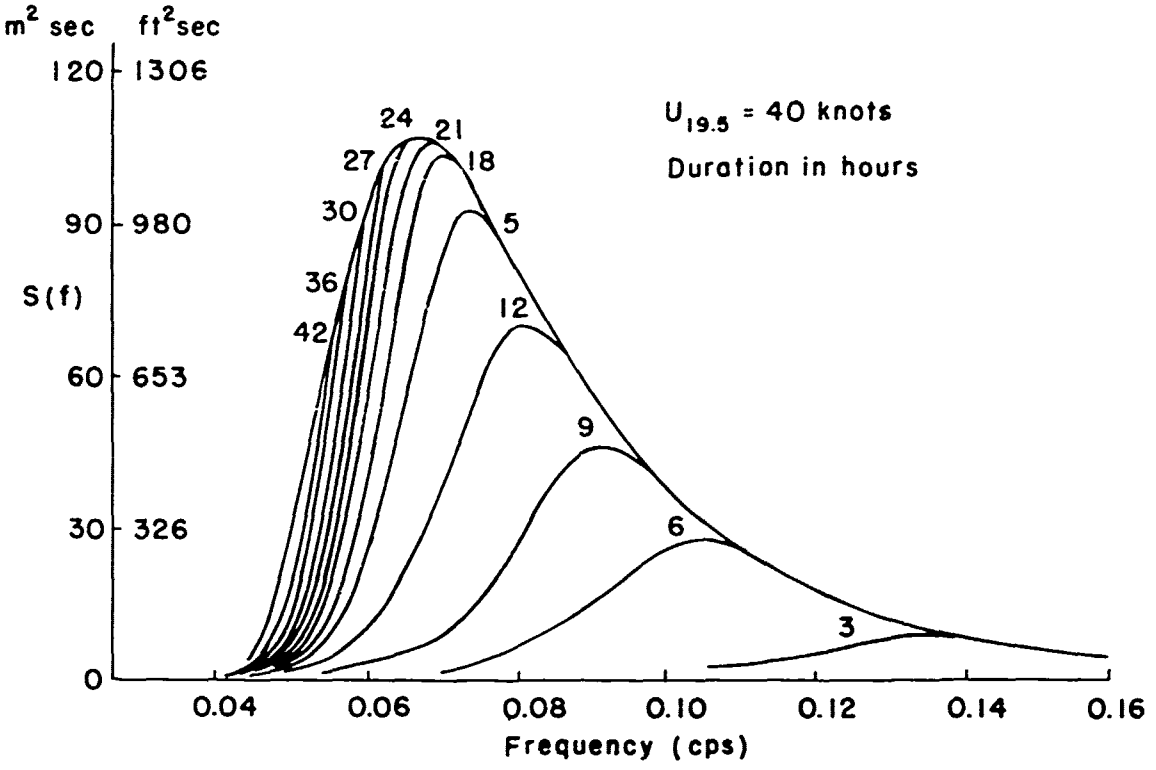

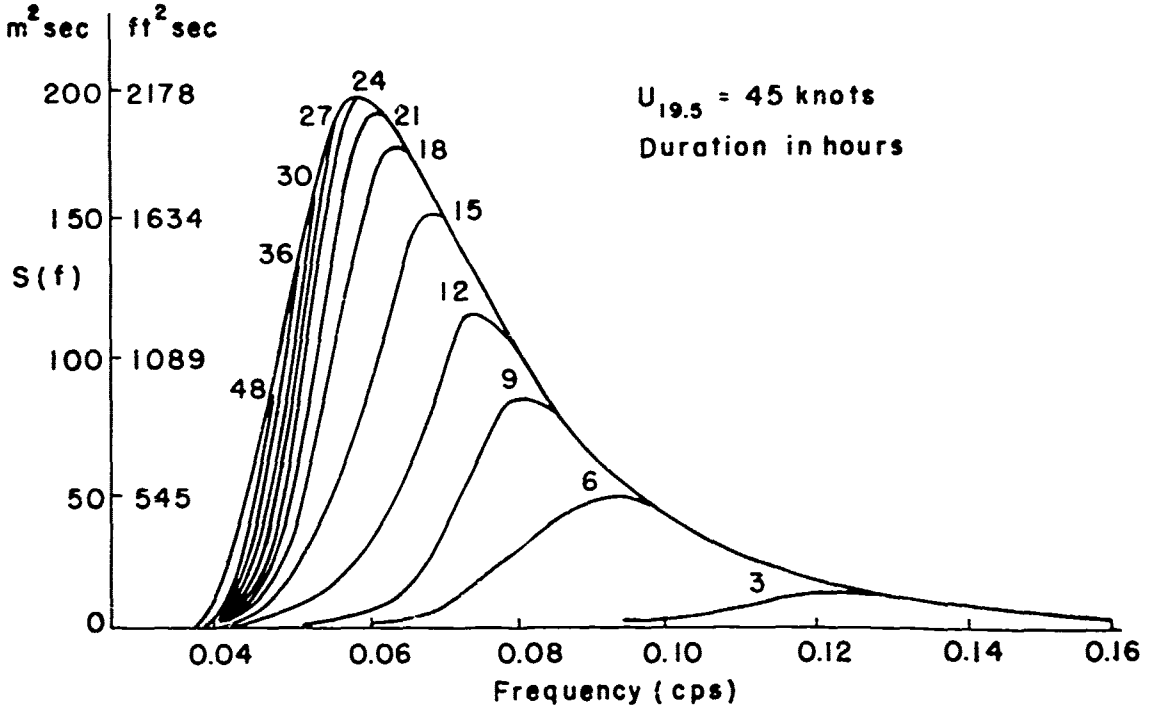

Figures 4e and 4f Growth of the spectrum for 40 and 45 knot winds with duration in hours.

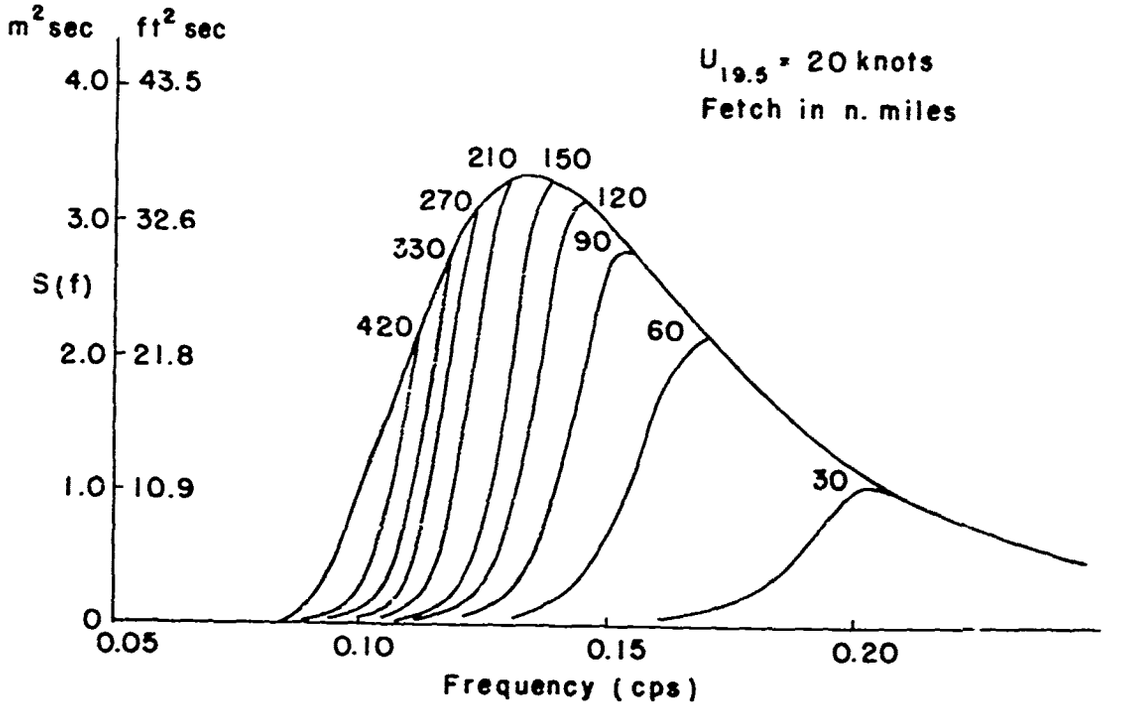

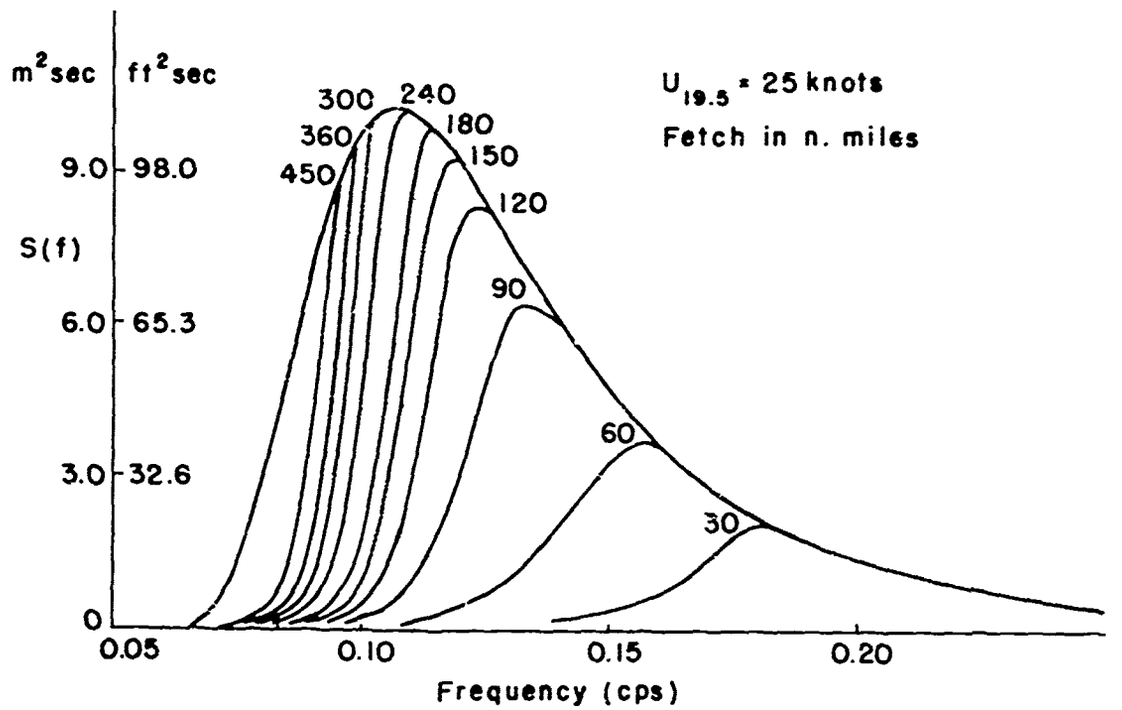

Figures 5a and 5b Growth of the spectrum for 20 and 25 knot winds with fetch in nautical miles.

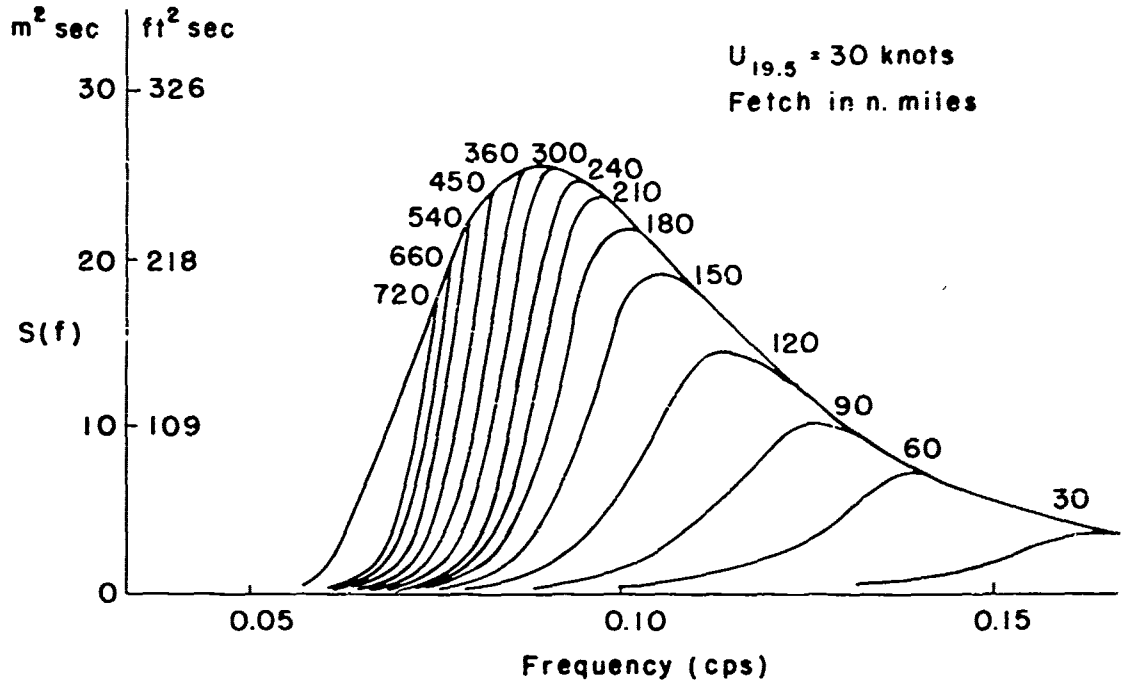

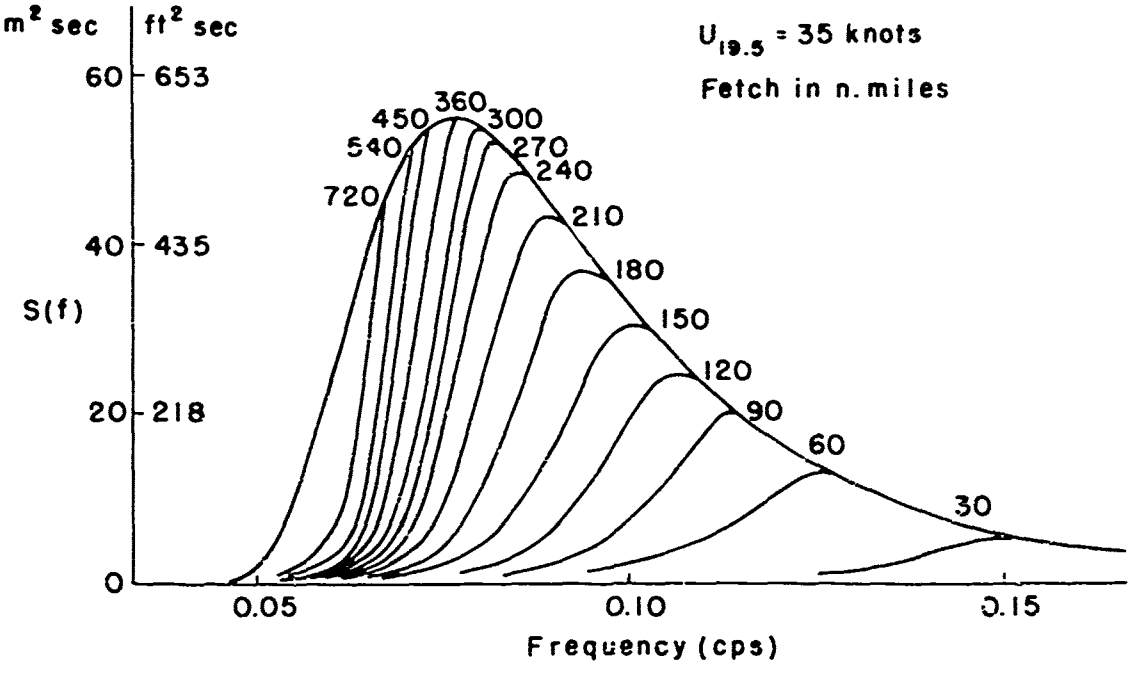

Figures 5c and 5d Growth of the spectrum for 30 and 35 knot winds with fetch in nautical miles.

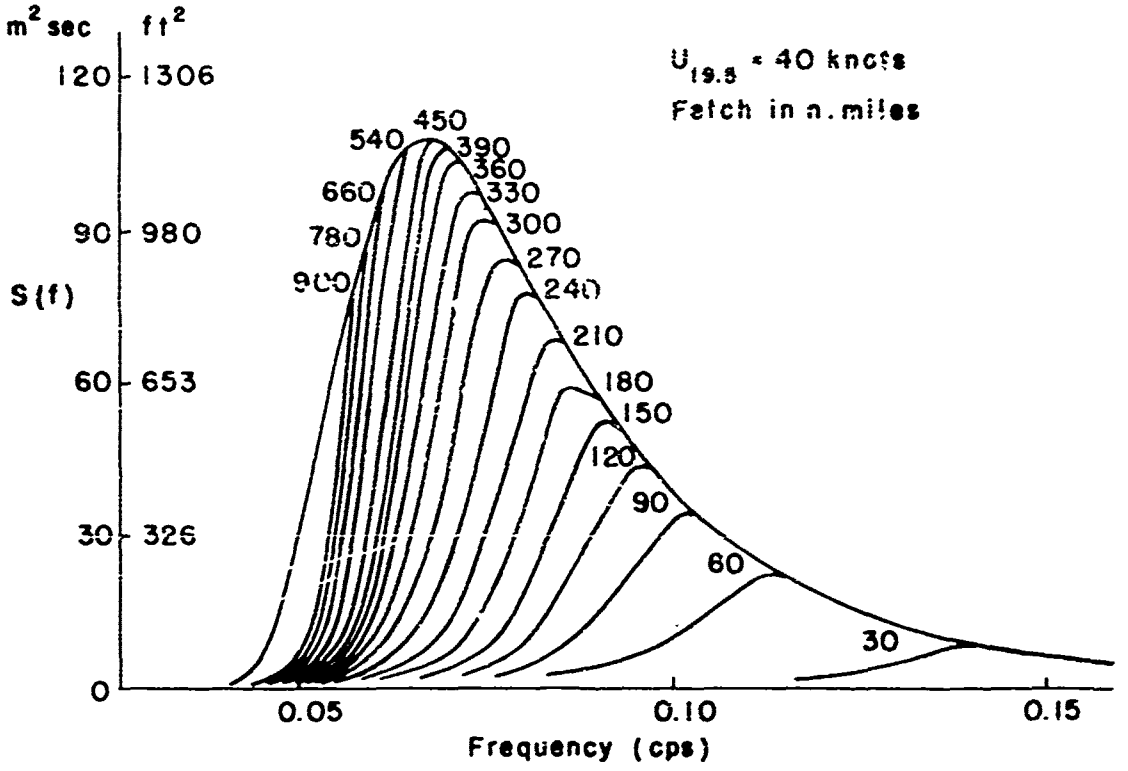

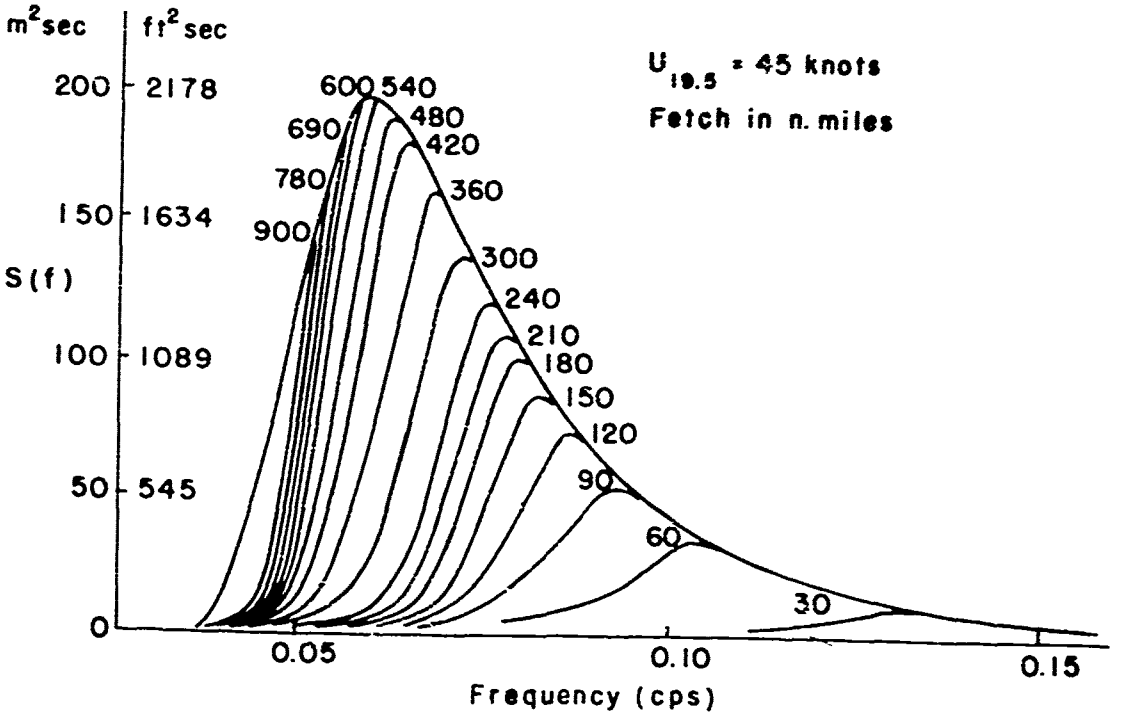

Figures 5e and 5f Growth of the spectrum for 40 and 45 knot winds with fetch in nautical miles.

equation was verified by using observations representing a rather wide range of sea conditions. However, none of these observations (including any of the other published observations of the drag coefficient c_{10} for high wind speeds) are representative of sea states for fully developed seas. When equation (5.6) is applied to spectra growing in these final stages, $\tilde{c}$ is very close to the wind speed, $\bar{u}$, and the corresponding drag coefficient approaches very low values. To check this tendency, a reasonable lower limit of 0.0007 was set at the ratio $u_*/u = \sqrt{c_{10}}$. Figures 4 and 5 were computed with this assumption.

In these figures, the spectra develop rapidly over the high frequency region in their early stages. This trend happens for all wind speed cases. For frequencies near the peak of the fully developed sea spectra, the pace of the spectral growth decreases. When the average phase speed $\tilde{c}$ comes close to the wind speed $\bar{u}$, the friction velocity decreases, and the growth rate of equation (5.9) also decreases in a general sense. Therefore, less energy is going to be fed in from the atmosphere to the waves in comparison with the energy input in the earlier stages. In this sense, then, the growth of the spectrum depends on the past stages of the growth and on the frequencies already present in the spectrum. This can be interpreted in terms of the fact that the instability mechanism growth is not so dominant in the low frequency region, and therefore, it takes a long time to reach the fully developed stage. This tendency occurs also for fetch spectral growth with respect to distance.

The spectral form of the partially developed sea shows a leading forward slope of the spectra that is not very steep for the early stages or for short fetches. Then the forward face becomes steeper while the spectra grow in the lower frequency range. As mentioned previously, this is the effect of the low growth rate of the instability mechanism at those frequencies. In figure 6, the spectra computed from the theoretical instability growth rate (4.18) are shown.

7. Comparison with other proposed spectra and spectral growth rates

Many theories have appeared since the beginning of the study of actual ocean wave generation. First, the parameters of the sea were computed by the non-dimensional method (Sverdrup and Munk, 1947; Bretschneider, 1957). After the concept of the spectra was introduced, wave observations were made from the spectral point of view, and many spectral forms were proposed (Neumann, 1953; Pierson, Neumann, and James, 1955; Darbyshire, 1955, 1959; Gelci, Cazale, and Vassal, 1957; Bretschneider, 1959). Directional spectra were observed by Cotê et al (1960), and Longuet-Higgins et al (1963). Walden (1963) gave a review of the differences among these proposed wave spectra. Later Pierson and Moskowitz (1964) proposed a form for fully developed sea spectra based on a similarity theory.

As the first step, fully developed sea spectra were studied more than the partially developed sea spectra. When forms of the spectra are compared, the spectra proposed by Darbyshire and Gelci et al (DSA II) show smaller spectral densities than the other

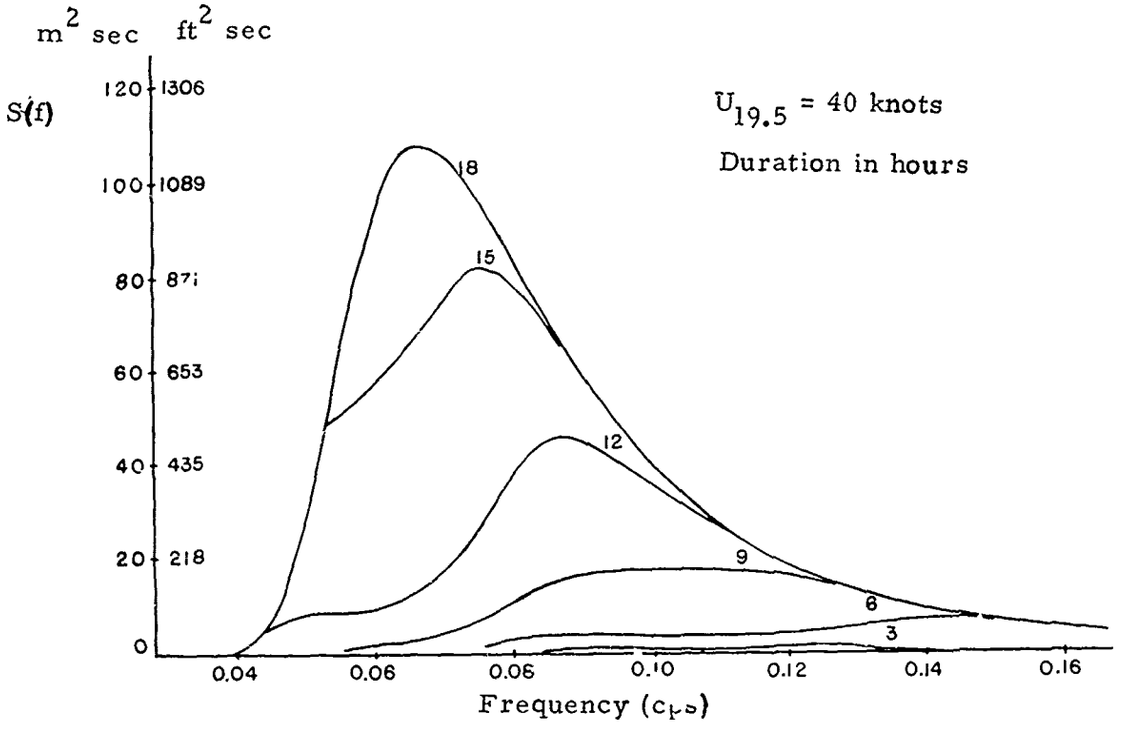

Figure 6 Growth of the spectrum with duration for a 40 knot wind speed in terms of the theoretical instability growth rate $B(f,u_*)$, instead of the proposed growth rate.

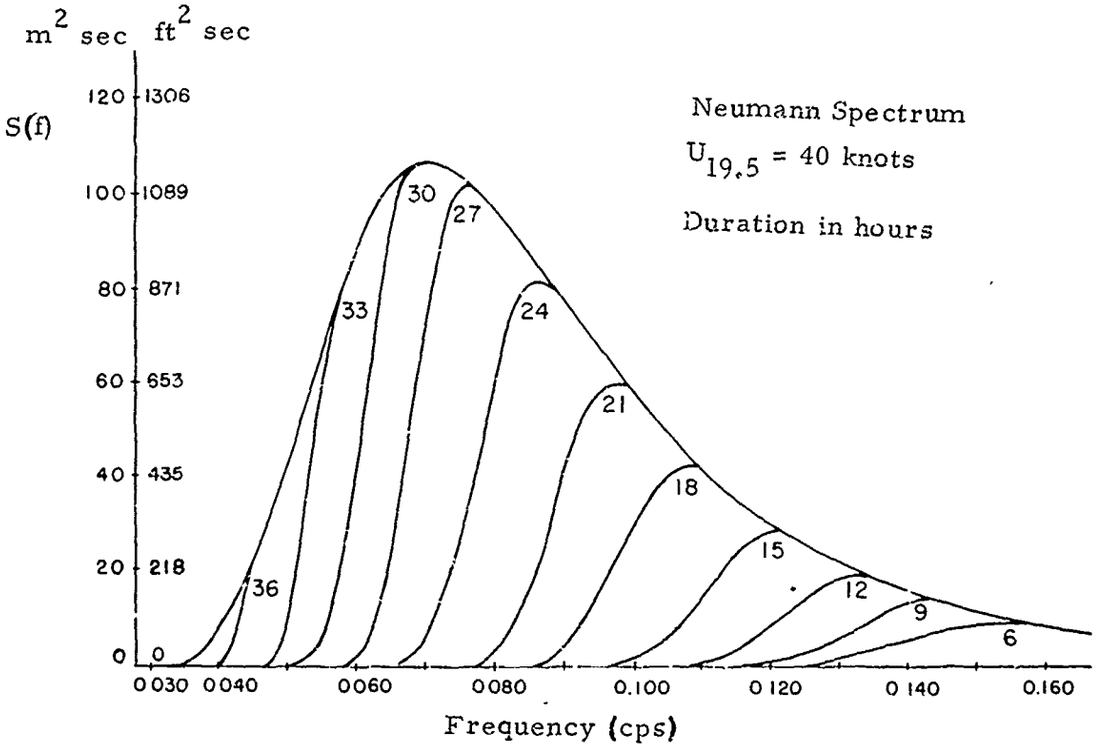

Figure 7 Growth of the spectrum with duration for a 40 knot wind

proposed spectra over the entire range of frequencies. It is not easy to compare these spectra because many different factors such as geographical conditions and differences in instrumentation are involved. One reason for the discrepancies, investigated by Pierson (1964), was the wind speed variation as a function of height. Pierson obtained closer agreement among the different proposals by Neumann, Wilson, and Pierson and Moskowitz.

In figure 7, the spectral growth for a 40 knot wind at 19.5 m by the PNJ method is shown. Pierson (1964) compared the fully developed sea spectra given by Neumann (1953) and by Pierson and Moskowitz (1964), and found them to be similar. Partially developed sea spectra in this study grow very fast for 0 to 15 hour durations over the higher frequency range, and the spectra pass the peak of the fully developed sea spectra after 24 hours from a zero initial spectrum. According to the PNJ method (H. O Pub. 603), the location of the forward edge of the spectrum is shown approximately, so the partially developed sea spectra in figure 7 are approximated by their leading edges. Generally, the partially developed sea spectrum of the PNJ method develops steadily toward the lower frequency range, and it fills the fully developed sea spectrum after a 36 hour duration. The spectrum of this study grows fast in the early stage, but does not attain the fully developed sea spectrum easily in the low frequency range. If the final stage of the development is neglected, it is considered that the spectrum reaches a fully developed sea after 40 hours.

When there is a big difference in the spectral growth theories,

the growth of some sea state parameters must be investigated. The significant wave height $\overline{H}_{\frac{1}{3}}$ as a function of the total energy of the sea may be an appropriate one to check wave growth. The significant wave height is plotted as a function of duration or fetch in figures 8(a) and 8(b). This significant wave height $\overline{H}_{\frac{1}{3}} = 2.83\sqrt{E}$, where E is twice the variance of the spectrum. In the same figures, the growth of $\overline{H}_{\frac{1}{3}}$ obtained by Sverdrup and Munk (1947) and PNJ (1955) are also shown for wind speeds of 20, 30, and 40 knots at 19.5 m.* The growth of the significant wave height proposed by Sverdrup and Munk fits very well for 20 and 30 knot winds in the duration growth graph 8(a). The wind speed applied was corrected to the value at the height of 19.5 m by using the drag coefficient proposed by Deacon and Webb (1962) from 10 m for Sverdrup and Munk's growth, and from 7.5 m for the PNJ method growth. However, the fetchwise growth of this study is more like the PNJ method than the Sverdrup-Munk method.

The growth rate of $\overline{H}_{\frac{1}{3}}$ by the PNJ method increases more slowly than this proposed growth. This is clear from the partially developed sea growth in figures 4 and 5. Similar figures for 40 knot winds significant wave height growth are shown by Walden (1963) and Wilson (1965) with many other proposed growth curves. However, the height at which wind speed was measured is not clearly specified in these growth rates. There are many variations in these figures. Generally, there are two growth rate groups. One

---

*Early definitions of significant height were, of course, not this precise.

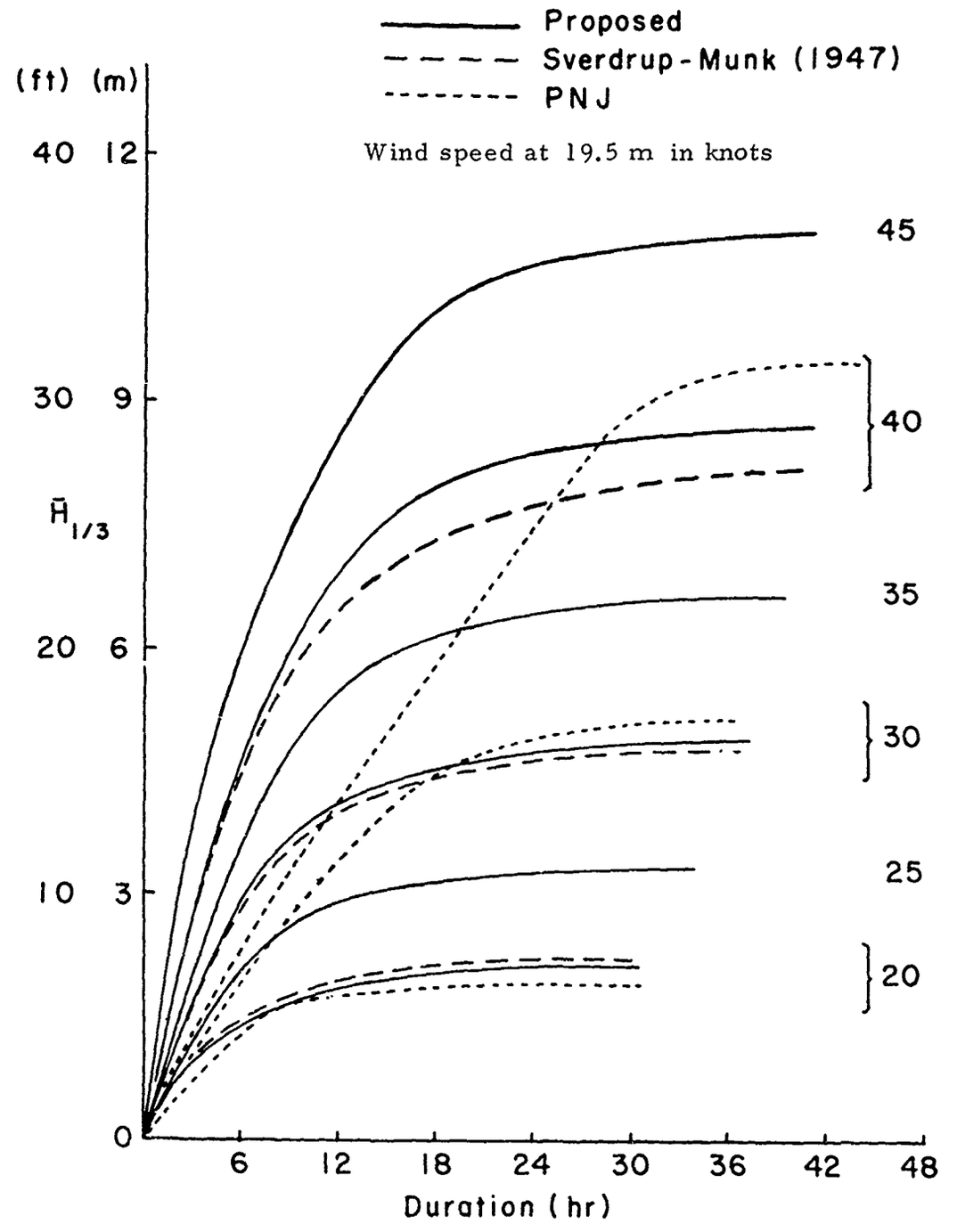

Figure 8a

Significant wave height growth versus duration for the Sverdrup-Munk method, the PNJ method, and the present method for different wind speeds.

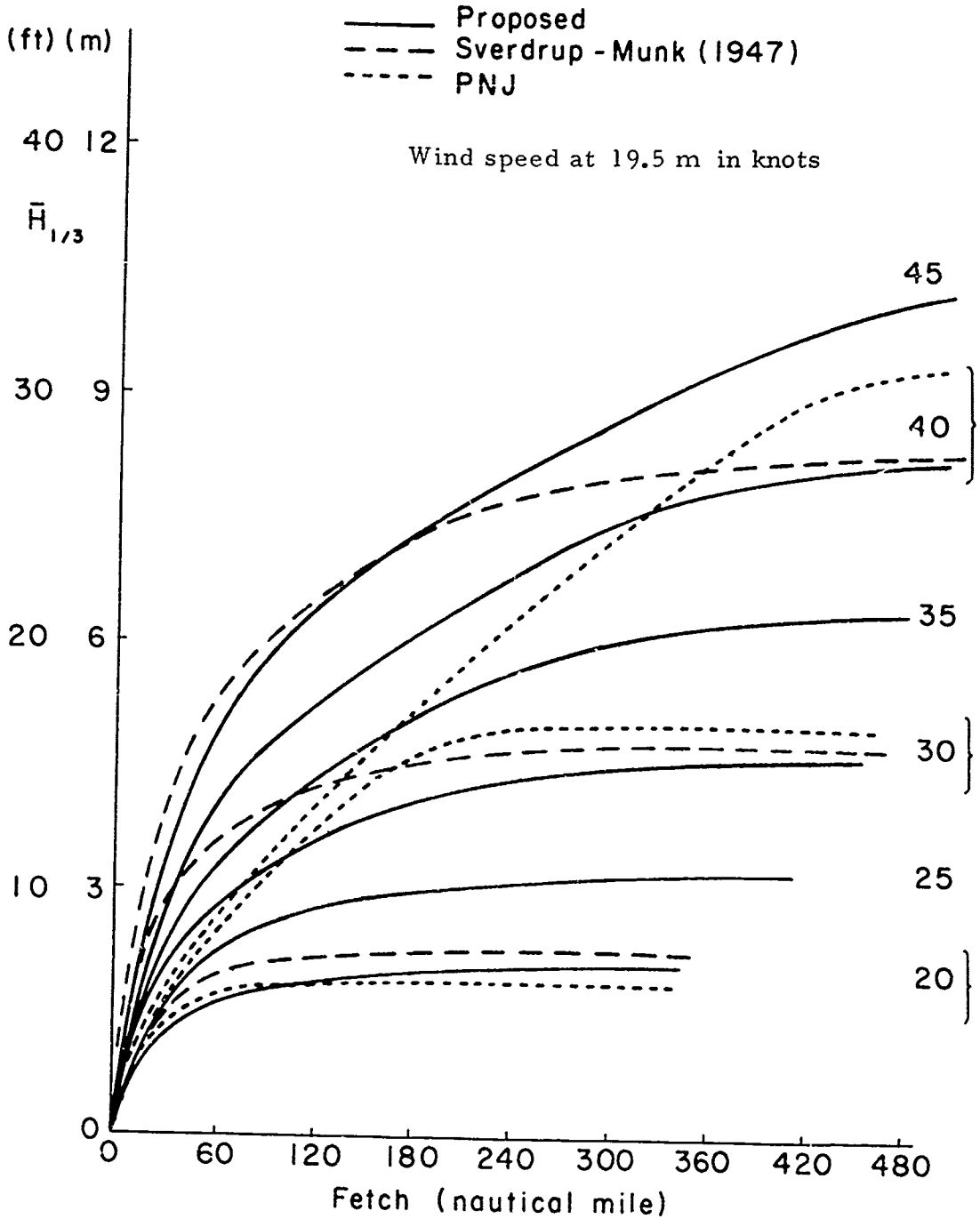

Figure 8b

Significant wave height growth versus fetch for the Sverdrup-Munk method, the PNJ method, and the present method for different wind speeds.

group shows a fast growing sea, and the other shows relatively slow growth.

One of the most distinctive points is the growth of the significant wave height proposed by Darbyshire. According to his study, the sea reaches the fully developed state easily for any wind speed. 100 to 150 nautical miles as a fetch, and 10 to 15 hours as a duration are said to be enough. On the contrary, 500 or more nautical miles and 36 hours are needed for the 40 knot wind speed spectra with the PNJ method.

There may be two reasons for considering a short fetch requirement for fully developed seas. One reason is as follows. When a wind field itself is moving with the same velocity as the propagation speed of the wave energy in the direction of the waves, then the waves can grow considerably higher even for a short apparent fetch. The second reason is the geographical location of the observation point. If the observation point is exposed to waves that are propagating from other areas, it is hardly possible for that location to be glassy calm. The weather ship stations in the North Atlantic can be considered to be locations such as this. While the sea always has some energy, an initial excitation due to the resonance mechanism is no longer needed, and so the sea grows in an exponential manner immediately and the duration required to reach a fully developed state becomes small. In an actual ocean, the two reasons mentioned above may occur simultaneously.

Suppose there exists some background sea. The spectrum grows faster and so does the wave height. To investigate this back-

COLUMBIA UNIVERSITY
HUDSON LABORATORIES
CONTRACT Nonr 266(84)

ground sea effect, the background sea level was assumed white and given a variance of a 20 knot wind sea. Furthermore, before strong winds of 40 or 50 knots blow, some weaker wind has already occurred, and a spectrum that is equivalent to the fully developed sea spectrum for 10 knots is supposed to exist in addition to the white noise. The larger of the values from either the white noise or the 10 knot wind fully developed sea was used. The white noise variance was 0.011 $(ft)^2$ for a frequency band of 1/180 sec^{-1}. The growths of the partially developed sea spectra for 30 knots and 40 knots were computed as shown in figure 9(a) and figure 9(b) under the background sea assumption. The background level used is also indicated in figure 9(a), but not in 9(b), because the level is so small that it cannot be seen. Naturally, the spectrum started from the background sea grows faster and it reaches a fully developed state easily because the growth in the low frequencies is quite rapid.

The discussion of the growth for a very short fetch or very short duration may have no meaning in this study. Even if the spectral growth for a particular component is the same, the different ones proposed have different spectral forms. So the growth behavior of the significant wave height is also different. However, the above reasons for a faster growth in some theories may be valid.

One of the points that should be noted in this model is that a particular spectral component shows a different growth behavior even for the same significant wave height and the same wind speed. The spectral growth depends on the friction velocity and not simply on the wind speed, and so the spectrum grows at different rates, even for the same wind and the same wave height.

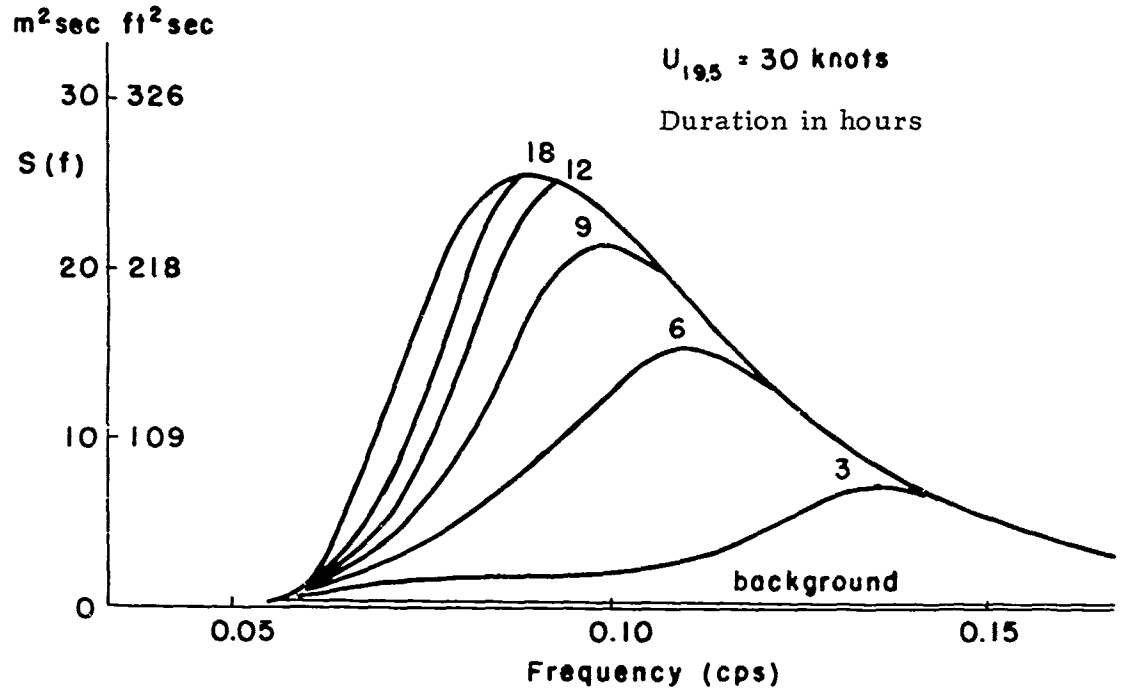

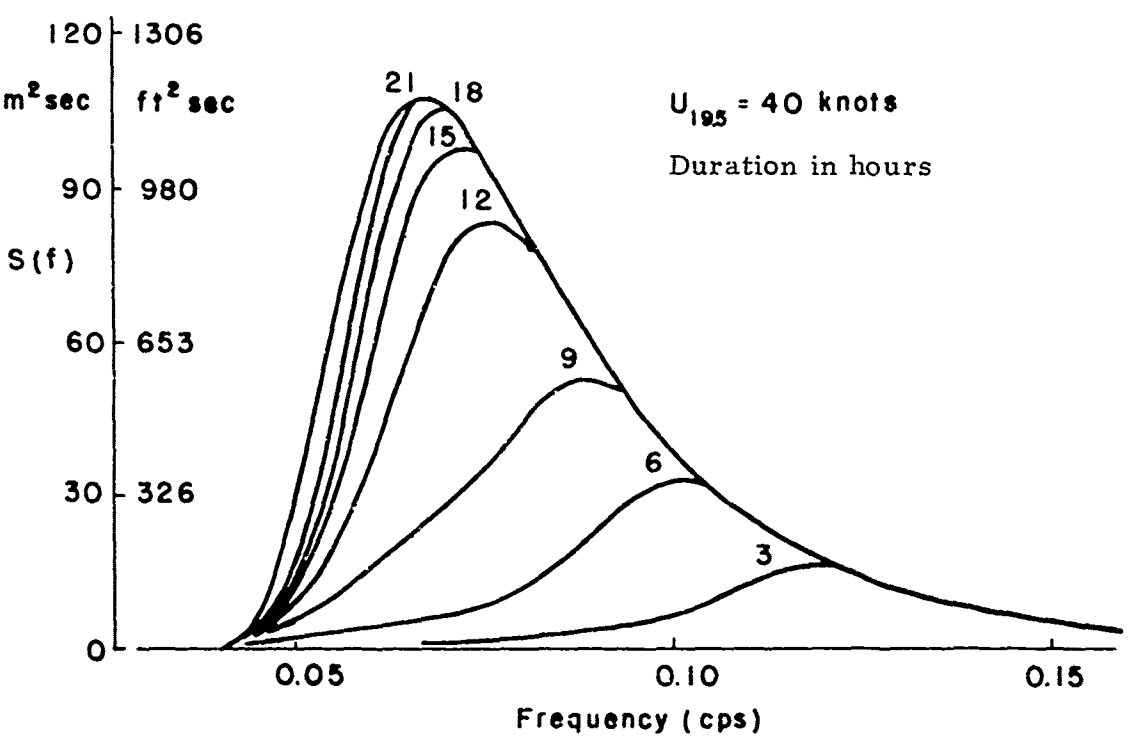

Figures 9a and 9b

Growth of the spectrum with duration for 30 and 40 knot winds with an estimated background sea already present (in the 40 knot wind case, the background sea level is too low to be plotted)

For example, consider the two different spectra described below. Suppose one spectrum has a steep forward slope that covers quite a narrow frequency band width. The other spectrum has a gentle forward slope that covers a wider frequency band. Then there exist two spectral components whose values are the same. However, the growths of these two spectral components are different because there are different friction velocities according to equation (5.6).

8. Application to forecasting

One of the purposes of ocean wave studies is to help forecast waves, and one object of this study is to improve wave forecasting methods. Therefore, computations by using this model must be compared with sea conditions that actually existed. For that purpose, it is desirable to hindcast the waves over a wide area and pick one particular geographical point to check the computed result.

Since the high speed computer has become available, the study of wave forecasting has been possible over wide ocean areas, and has shown remarkable progress. Baer (1962) studied wave forecasting methods in the North Atlantic, and used 519 grid points which were roughly 120 nautical miles apart over the whole North Atlantic Ocean. At that time, the change of the quantity, E, was tabulated per unit time interval by using the PNJ method, and the growth of the following time steps was obtained from that growth table. Many parts of the program were revised later, and the details of the numerical procedure were given in other publications (Pierson, 1964; Pierson, Tick and Baer, 1966; Bunting, 1966).

The essence of this process is described below.

First of all, the wind field must be determined. The regression equation given by Thomasell and Welsh (1963) is used to guess the first wind field from the surface pressure field. This estimate, then, is corrected by using the observed wind data obtained by weather ships, navy ships, and other commercial ships with priority in this order. The wind speeds are referred to a 19.5 m height which is the British weather ships' anemometer height by assuming the wind profile to be logarithmic. The wind profile is obtained in the JNWP grid system, and is interpolated into the 519 grid point system mentioned above (Baer, 1962).

The growth of the spectra for three-hour intervals is computed under the wind field obtained. Equation (6.3) is used for fully developed sea spectra. When the spectra at each time are below the fully developed spectral component value, further growth is allowed. The spectral growth model of this study is applied to a growth instead of the E growth table. The forecasts (or hindcasts in this study) of the spectra are made for fifteen frequency bands to make computation faster. The following frequency bands were chosen [unit is cycles per second].

0.036 - 0.042,	0.042 - 0.047 ,	0.047 - 0.053 ,
0.053 - 0.058,	0.058 - 0.064 ,	0.064 - 0.069 ,
0.069 - 0.075,	0.075 - 0.080 ,	0.080 - 0.086 ,
0.086 - 0.097 ,	0.097 - 0.108 ,	0.108 - 0.125 ,
0.125 - 0.142 ,	0.142 - 0.164 ,	0.164 - ∞

In the fifteenth band, the sea is estimated to be always fully developed since the high frequencies easily reach the fully developed sea spectrum. Thus, the fully developed spectral value is applied to that band instead of computing a growth. The functions for A in equation (6.6) and for B in equation (6.7), must be obtained first, and the A term is simply a function of wind speed and frequency. The B function depends on a friction velocity u_*, and u_* should be computed from equation (5.6). Thus, before computing the spectral growth, the sea conditions, $\overline{H}_{\frac{1}{3}}$ and $\tilde{c}$, must be obtained for the grid point concerned. When an average $\tilde{c}$ is computed, the quantity $f^2S(f)$ is needed. The center frequency f_c of the band is used and $f_c^2 S(f_c)$ is applied even for the broader frequency band except the fifteenth frequency band (0.164 cps $\sim \infty$).

The friction velocity, u_*, for each grid point is obtained from the initial sea state, and the spectral component growth for three hours is computed by using this model. The spectrum obtained in such a way is a one-dimensional spectrum, so the equation derived by the SWOP project (Coté et al, 1960) is used to obtain the directional spectra. The formula is

$$F(\omega, \theta, u) = \frac{1}{\pi}\left[1 + \left(0.50 + 0.82\, e^{-\frac{1}{2}(\omega u/g)^4}\right)\cos 2\theta + 0.32\, e^{-\frac{1}{2}(\omega u/g)^4}\cos 4\theta\right] \qquad (8.1)$$

for $-\frac{\pi}{2} < \theta < \frac{\pi}{2}$, and $F(\omega, \theta, u) = 0$, elsewhere. θ is the angle between the wind direction and the direction of the wave component. The directional spectra are computed for 30° angular bands. As a result, the spectra are shown by 180 spectral components

(15 frequency bands) x (12 directional bands). The spectral values are propagated at group velocity in their appropriate direction.

While the wave grows and propagates, the wave may also dissipate in its travels. The spectral component can be considered not to receive any energy but to dissipate when the wave moves against the wind. In this forecasting procedure, the dissipation rate is assumed to be a function of the total energy of the wind sea traveling within 90° to the wind direction, and the fourth power of its component's frequency.

$$S_D(f_i, \theta_i) = S_o(f_i, \theta_i)\left[e^{-c\sqrt{S_w}\, f_i^4} \right]^{k(\theta_1)} \qquad (8.2)$$

where

$S_D(f_i, \theta_i)$ = spectral component after dissipation

$S_o(f_i, \theta_i)$ = spectral component before dissipation

f_i, θ_i = center frequency and direction of that component

c = constant 690 (for ft^2), 169.2 (for $m^2 sec$)

S_w = $\Sigma\Sigma S_w(f_i, \theta_i)$

and

$k(\theta_1)$ = 0 for $\theta_1 \leq 75°$

$k(\theta_1)$ = 1.5 for $75° < \theta_1 \leq 105°$

$k(\theta_1)$ = 3.0 for $105° < \theta_1 \leq 135°$

$k(\theta_1)$ = 4.5 for $135° < \theta_1 \leq 165°$

$k(\theta_1)$ = 6.0 for $165° < \theta_1 \leq 180°$

Thus, the spectral components computed at a grid point transfer some energy to the other grid points, receive energy from the other grid points, and combine to form a new sea state. The next time step

computation is repeated from this new sea condition, and the result is recorded every six hours.

Wave hindcasts for December 1959 were made for the North Atlantic as a test. In the second half of December 1959, three big storms attacked the northern part of that ocean. The meteorological and sea conditions are discussed in detail by Bretschneider et al (1962). Within half a month, significant wave heights of forty feet were observed twice, and a wind speed of more than 60 knots was observed at times on the weather ship located at "J". The corresponding changes of the wave height, which accompanied the changes of the wind speed, can be thought to be the best sample for checking this growth model by using the forecasting procedure mentioned above.

The wind field used in this test was derived by the regression equation from the pressure pattern, and corrected by the ship's data. Thus there were some differences between the actual wind field and the input wind field, and also the grid point chosen was not at the same location as the weather ship. The observed wind velocities and the hindcasted wind velocities are listed in Appendix III. Atmospheric stability was not taken into account in this study, so the air-sea temperature difference effect was neglected.

The computation starts from a zero initial sea condition, but there are enough days to produce a sea state that is close to the actual sea condition before 16 December. The computation began eight days prior to 16 December. The time history of the hindcasted significant wave height at the two grid points closest to weather ship J is shown in figure 10. The relative position to J is seen in that figure.

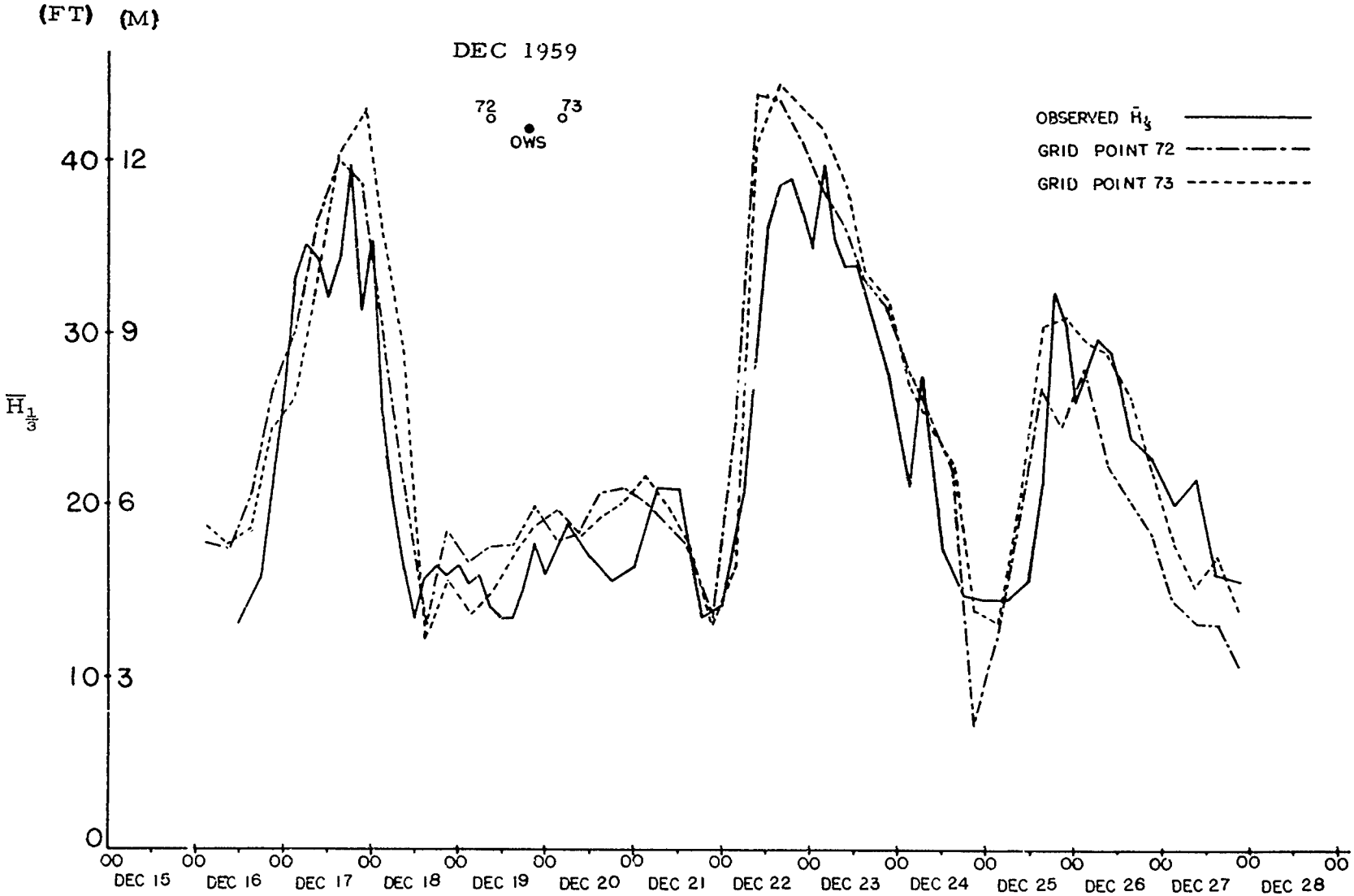

Figure 10 Observed and hindcasted significant wave heights versus time (GMT), Dec., 1959, at and near the weather station J in the North Atlantic.

Although there are some differences between the observed and hindcasted significant wave heights, these hindcasted values follow the observed ones fairly well. The bias of the wave height is + 0.4 m (+1.3 ft) and the RMS error is 1.6 m (4.9 ft) for grid point 72, and +0.7 m (2.1 ft) and 1.4 m (4.3 ft), respectively, for grid point 73.

The purpose of this wave forecasting study is not only to predict significant wave height, but also to predict spectra close to the actual ones observed. Therefore, the investigation must be extended to the form of the spectra or to the spectral components changing with time. The study to check how the ocean wave spectra can be reproduced is important for practical purposes such as ship motions in waves. The one-dimensional spectra were obtained to study the growth and decay of the spectral components.

Although fifteen frequency bands were computed, only six low frequency bands are shown in figure 11. The spectral components in the higher frequency bands showed growth and decay that agreed well with the observations, and a problem remained in the low frequency range only. When the old growth model (Inoue, 1966) was used, there was no reproduction of spectral components that appeared in the low frequencies. But in this model, even in the lowest frequency, f = 0.039 (cps), the spectral component was reproduced quite well. This low frequency component prediction is considered to be the effect of the undulatory turbulent flow induced mainly by the waves. The hindcasted components seem to grow a little too fast, although they do not decrease fast enough after the storm for f = 0.055, 0.050, and 0.045 cps. The results could not

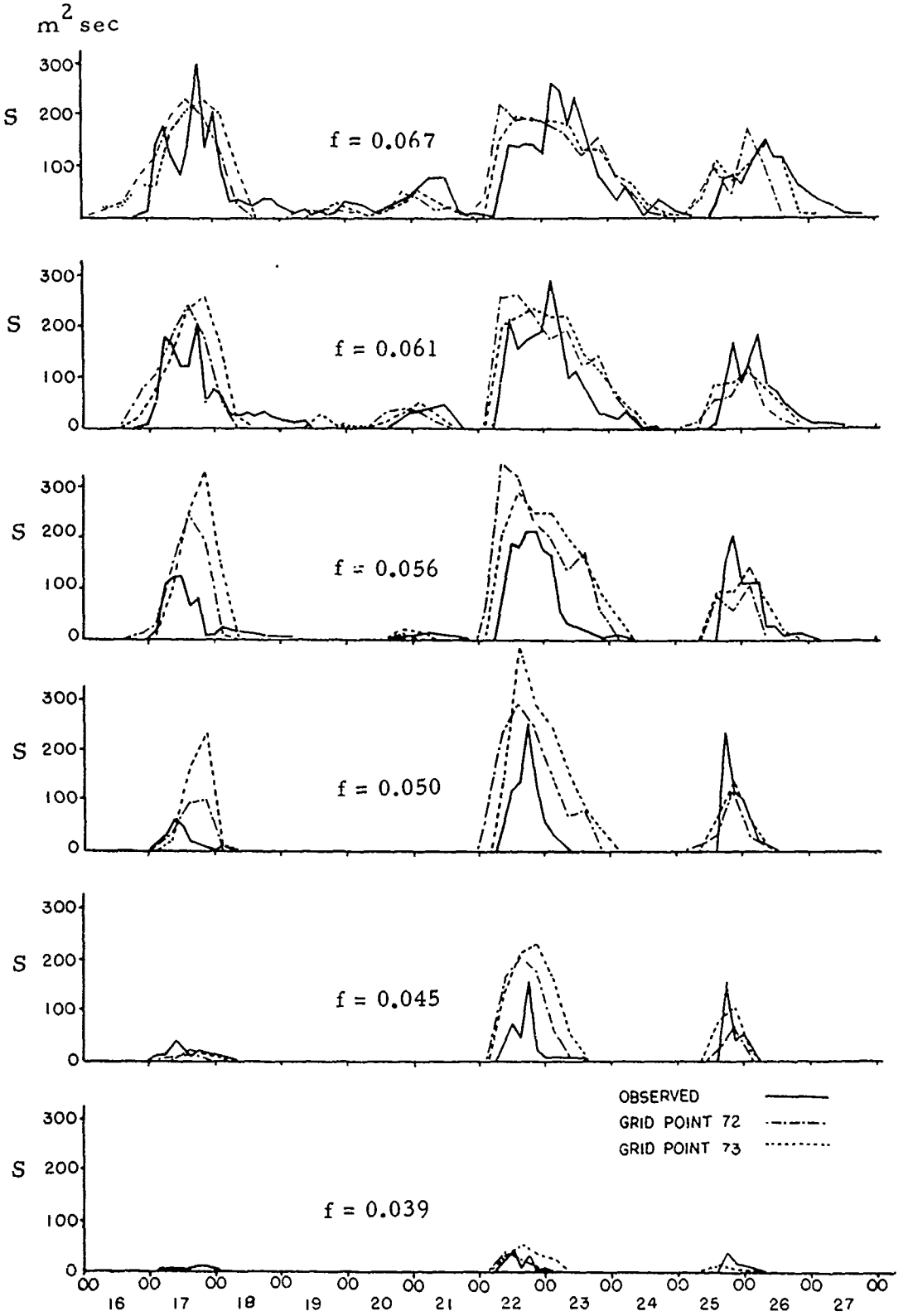

Figure 11 Observed and hindcasted spectral densities for different frequency components versus time (GMT), Dec., 1959, at and near the weather station J in the North

be further refined without investigating the actual wind field in detail over the whole North Atlantic. As far as the low frequency part of the spectrum is concerned, the growth rate of this study improved the forecasting results.

Hindcasts of ocean waves were also made for 20 November through 30 November 1961. During this period, wave observations were made at the Argus Island tower and analyzed by Pickett (1962). The meteorological and wave situations were also discussed by De Leonibus (1962) as well as the wave hindcasts obtained by using the PNJ method. The hindcasted significant wave heights for the two grid points nearest to the tower are shown in figure 12 along with the observed significant heights. The procedure for the computation is the same as the December 1959 case except for the wind field used, which was analyzed manually [provided by L. Moskowitz*]. Although there are differences at the two grid points due to the complicated weather situation for the first half of the period, the most interesting hindcasts occurred on 25, 27, and 28 November. These rapid wave height changes have never been reproduced before. The bias and the RMS error for grid point 229 are respectively, -0.53 m (-1.59 ft) and 1.25 m (3.76 ft); for grid point 230 they are -0.17 m (-0.57 ft) and 0.93 m (3.10 ft). Generally speaking, the hindcasts from this study are more sensitive to the meteorological and sea conditions in comparison to the growth table method and the old model (Inoue, 1966). This is one of the distinguishing characteristics of this procedure.

*U. S. Naval Oceanographic Office.

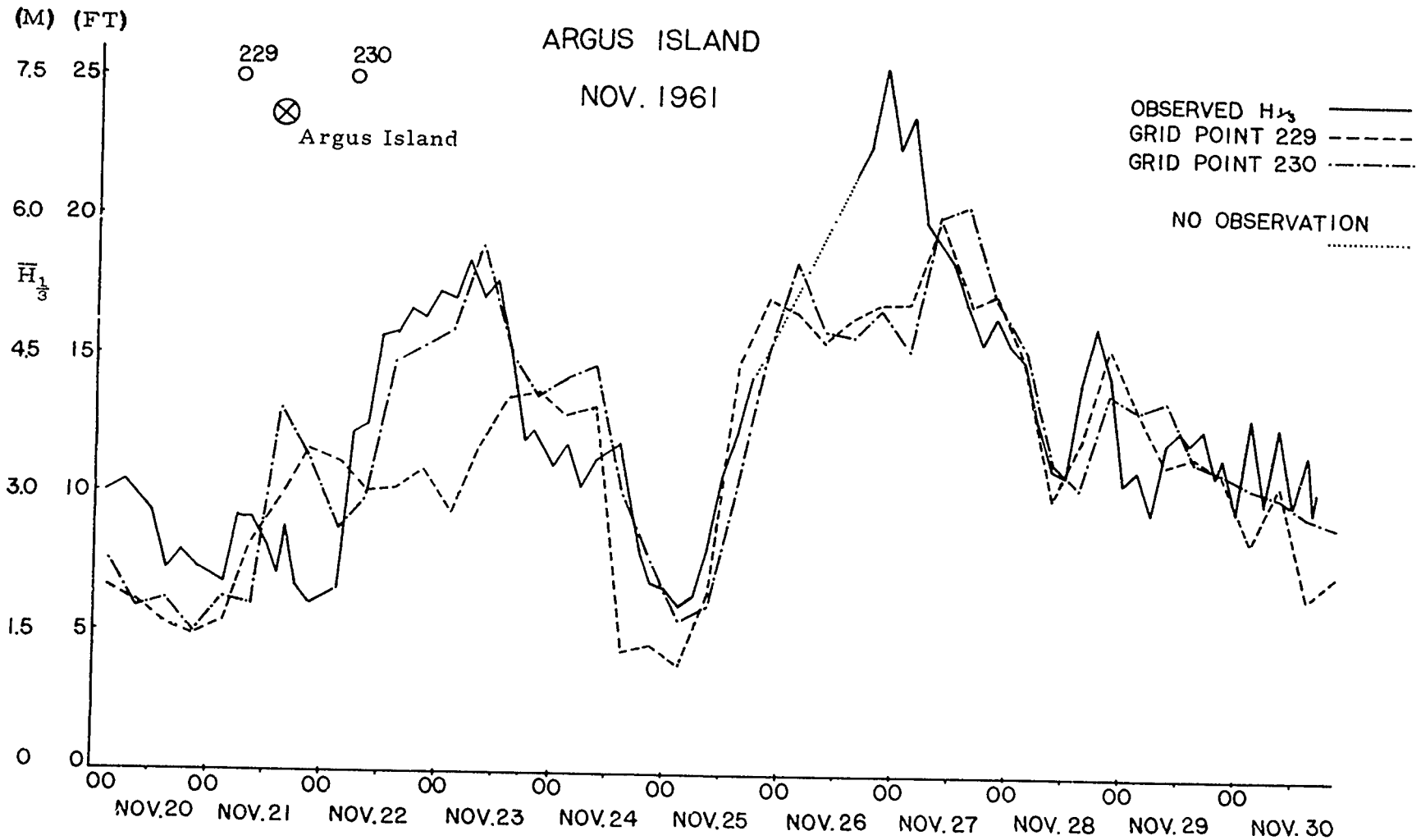

Figure 12. Observed and hindcasted significant wave heights versus time, Nov. 1961, at and near the Argus Island tower.

9. Conclusions

Observations showed an irregular trend in the figure of instability mechanism growth, as shown in figure 3. This "bump" had not been explained sufficiently. Although there are discrepancies between observed growth rates and theoretical values in the high and also low ranges of u_*/c, the new theory proposed by Phillips can explain the existence of the "bump" in figure 3. The growth rate is a function of u_*/c, and the friction velocity, u_*, should be determined. The relation between the roughness parameter and the sea state was found by Kitaigorodskii and Volkov, and this relation was applied to the computation of the friction velocity.

Therefore, the friction velocity is a function of the sea state, or the average phase speed and the wave height, and so is the growth rate, B/f. Even for the same wind speed at 19.5 meters, the growth rate for a particular component is not the same, but depends on the sea state. Physically, this can be interpreted to mean that less energy can be fed in by an instability process, while the waves are growing and moving with the wind.

The proposed sea spectra growth shows faster development in an early growing stage (or short fetch), and slower growth in the last stages. It takes from 35 to 40 hours or from 700 to 1000 nautical miles to reach a fully developed sea for a 40 knot wind. This growth rate of the significant wave height is almost the same as the results of Sverdrup and Munk for duration, but for fetch the growth is slower. The durations and fetches required to reach fully developed seas seem larger in comparison to the other proposed values

such as those of Darbyshire. The discrepancies may be explained by the existence of a background sea.

The formulas obtained in this study were used in a wave forecasting computer program. The hindcasted significant wave height shows good agreement with the observed heights at weather station J in the North Atlantic for the second half of December 1959.

Spectral components were also investigated for low frequency ranges which had not been properly described in an earlier model. The spectral components in that region also showed better growth. Although this is a linear model basically and the atmospheric stability was assumed to be neutral, the results can be said to be satisfactory.

References

Baer, L. (1962): An experiment in numerical forecasting of deep water ocean waves. Lockheed Missile and Space Co., Sunnyvale, Calif.

Barnett, T.P. (1967): On the generation, dissipation, and prediction of ocean wind waves. U.S. Naval Oceanographic Office, Washington, D.C. 58 pp.

Barnett, T.P., and J.C. Wilkerson (1966): On the interpretation of fetch-limited wave spectra as measured by an airborne sea-swell recorder. U.S. Naval Oceanographic Office, TR-191, 60 pp.

Bretschneider, C.L. (1951): Revised wave forecasting curves and procedure. Tech. Report HE-155-47. Institute of Engineering Research, University of California, 28 pp.

Bretschneider, C.L. (1959): Wave variability and wave spectra for wind generated gravity waves. Beach Erosion Board Tech. Memo. No. 118.

Bretschneider, C.L., H.L. Crutcher, J. Darbyshire, G. Neumann, W.J. Pierson, Jr., and H. Walden (1962): Data for high wave conditions observed by the OWS "Weather Reporter" in December 1959. Deut. Hydrogr. Z., Band 15, Heft 6, pp. 243-255.

Bunting, D.C. (1966): Wave hindcast project- North Atlantic Ocean. Tech. Report TR-183, Oceanographic Analysis Division, U.S. Naval Oceanographic Office, Washington, D.C., 35 pp.

Charnock, H. (1955): Wind-stress on a water surface. Quart. J. Roy. Meteor. Soc., 81, 639.

Coté, L.J., J.O. Davis, W. Marks, R.J. McGough, E. Mehr, W.J. Pierson, Jr., F.J. Ropek, G. Stephenson, and R.C. Vetter (1960): The directional spectrum of a wind generated sea as determined from data obtained by the Stereo Wave Observation Project. Meteor. Pap., Vol. 2, No. 6, 88 pp. New York University Press, (New York).

Darbyshire, J. (1955): An investigation of storm waves in the North Atlantic Ocean. Proc. Roy. Soc., A, Vol. 230, No. 1183, pp. 560-569.

Darbyshire, J. (1959): A further investigation of wind generated waves. Deut. Hydrogr. Z., Band 12, Heft 1, pp. 1-13.

Deacon, E.L., and E.K. Webb (1962): Small-scale interactions. The Sea, Vol. 1, pp. 43-87. Interscience Publishers, New York.

DeLeonibus, P.S. (1962): Comparison of hindcast to observed significant wave heights at Argus Island November 20 to 30, 1961. Marine Sciences Dept., U S. Naval Oceanographic Office, 30 pp. (unpublished)

Gelci, R., H. Cazalé, and J. Vassal (1957): Prévision de la houle, la méthode de densités spectro-angulaire. Extrait du Bulletin d'Information du Comité Centrale d'Océanographie, 9(8), pp. 416-435.

Hasselmann, K. (1962): On the non-linear energy transfer in the gravity wave spectrum, Part I. J. Fluid Mech., 12, pp. 481-500.

Hasselmann, K. (1963a): On the non-linear energy transfer in the gravity wave spectrum, Part II. J. Fluid Mech., 15, pp. 273-281.

Hasselmann, K. (1963b): On the non-linear energy transfer in the gravity wave spectrum, Part III. J. Fluid Mech., 15, pp. 385-398.

Inoue, T. (1966): On the growth of the spectrum of a wind generated sea according to a modified Miles-Phillips mechanism. Geophysical Sciences Lab. Report No. TR 66-6, New York University, School of Engineering and Science, New York.

Inoue, T. (1967): Ocean wave spectra estimated from three hour pressure records obtained by FLIP. Geophysical Sciences Lab. Report No. TR 67-1, New York University, School of Engineering and Science, New York.

Jeffreys, H. (1925): On the formation of water waves by wind. Proc. Roy. Soc., A, 107(A742), 189-206.

Kitaigorodskii, S.A. (1961): Application of the theory of similarity to the analysis of wind generated wave motion as a stochastic process. Izv. Akad. Nauk. SSSR, Ser. Geofiz., Vol. 1, pp. 105-117 (English Transl. 1, pp. 73-80).

Kitaigorodskii, S.A., and Y.A. Volkov (1965): On the roughness parameter of the sea surface and the calculation of momentum flux in the near-water layer of the atmosphere. Izv. Akad. Nauk SSSR, Atmospheric and Oceanic Physics Series, Vol. 1, No. 9, pp. 973 (English translation).

Lamb, H. (1932): Hydrodynamics. 6th edition, Cambridge University Press .

Lighthill, M.J (1962): Physical interpretation of the mathematical theory of wave generation by wind. J. Fluid Mech., 14, pp. 385-397.

Longuet-Higgins, M.S (1952): On the statistical distribution of the heights of sea waves. J. Mar. Res., 11, pp. 245-266.

Longuet-Higgins, M S., D.E. Cartwright, and N.D. Smith (1963): Observations of the directional spectrum of sea waves using the motions of a floating buoy. Ocean Wave Spectra, pp. 111-131, Prentice-Hall, Englewood Cliffs.

Miles, J.W. (1957): On the generation of surface waves by shear flows. J. Fluid Mech., 3(2), pp. 185-204.

Miles, J.W. (1959): On the generation of surface waves by shear flows. Part II. J. Fluid Mech., 6(4), pp. 568-582.

Miles, J.W. (1960): On the generation of surface waves by turbulent shear flows. J. Fluid Mech., 7, pp. 469-478.

Moskowitz, L., W.J. Pierson, Jr., and E. Mehr (1962, 1963, 1965): Wave spectra estimated from wave records obtained by the OWS "Weather Explorer" and the OWS "Weather Reporter". Parts I, II, and III. Tech. Reports, New York University, School of Engineering and Science, Dept. of Meteor. and Oceanography.

Neumann, G. (1953): On ocean wave spectra and a new method of forecasting wind generated sea. Tech.Memo. No. 43, Beach Erosion Board, Corps of Engineers, Washington, D.C.

Neumann, G., and W.J. Pierson, Jr. (1963): Known and unknown properties of the frequency spectrum of a wind-generated sea. Ocean Wave Spectra, pp. 9-25, Prentice-Hall, Englewood Cliffs, New Jersey.

Ocean Wave Spectra (1963): Proceedings of a Conference Held at Easton.Maryland, May 1-4, 1961. 357 pp., Prentice-Hall, Englewood Cliffs, New Jersey.

Phillips, O.M. (1957): On the generation of waves by turbulent wind. J. Fluid Mech., 1(5), pp. 417-445.

Phillips, O.M. (1958): The equilibrium range in the spectrum of wind generated waves. J. Fluid Mech., 4(4), pp. 426-434.

Phillips, O.M. (1966): The Dynamics of the Upper Ocean. Cambridge Univ. Press, 261 pp.

Pickett, R.L. (1962): A series of wave power spectra. Marine Science Dept., U.S. Naval Oceanographic Office, Washington, D. C.,111 pp. [unpublished]

Pierson, W.J. (1964a): The interpretation of wave spectra in terms of the wind profile instead of the wind measured at a constant height. J. Geophys. Res., 69(24), pp. 5191-5203.

Pierson, W.J. (1964b): Known and unknown properties of the two-dimensional wave spectrum and attempts to forecast the two-dimensional wave spectrum for the North Atlantic. Proc. Fifth Symposium on Naval Hydrodynamics, Ship motions and drag reduction, Sept. 10-12, 1964, Bergen, Norway. ACR-112, Office of Naval Research, Washington, D.C., pp. 425-433.

Pierson, W.J., and L. Moskowitz (1964): A proposed spectral form for fully developed wind seas based on the similarity theory of S.A. Kitaigorodskii. J. Geophys. Res., 69(24), pp. 5181-5190.

Pierson, W.J., G. Neumann, and R.W. James (1955): Practical methods for observing and forecasting ocean waves by means of wave spectra and statistics. H.O Pub. 603, U.S. Navy Hydrographic Office, Washington, D.C.

Pierson, W.J., L.J. Tick, and L. Baer (1966): Computer based procedure for preparing global wave forecasts and wind field analysis capable of using wave data obtained by a spacecraft. 6th Naval Hydrodynamics Symposium, Sept. 28-Oct. 4, 1966, Washington, D.C., Vol. II, 20-1.

Priestly, J.T. (1966): Correlation studies of pressure fluctuations on the ground beneath a turbulent boundary layer. National Bureau of Standards, NBS Report 8942, 92 pp. U.S. Dept. of Commerce.

Shemdin, O.H., and E.Y. Hsu (1966): The dynamics of wind in the vicinity of progressive water waves. Tech. Report No. 66, Dept. of Civil Engineering, Stanford University, 209 pp.

Snodgrass, F.E., G.W. Groves, K.F. Hasselmann, G.R. Miller, W.H. Munk, and W.H. Powers (1966): Propagation of ocean swell across the Pacific. Phil. Trans. Roy. Soc. London, A, Vol. 259, No. 1103, pp. 431-497.

Snyder, R.L., and C.S. Cox (1966): A field study of the wind generation of ocean waves. J. Mar. Res., 24(2), pp. 141-177.

Sverdrup, H.U., and W.H. Munk (1947): Wind, Sea, and Swell: Theory of Relations for Forecasting. U.S. Hydrographic Office, H.O. Pub. 601, 44 pp.

Thomasell, A., and J.G. Welsh (1963): Studies of the specification of surface winds over the ocean. Final Report. The Travelers Research Center, Inc., Hartford, Conn.

Tucker, J. W. (1956): A ship-borne wave recorder. Trans. Inst. Naval Arch., Vol. 98, pp. 236-250.

Walden, H. (1963): Comparison of one-dimensional wave spectra recorded in the German bight with various "theoretical" spectra. Ocean Wave Spectra, pp. 67-81, Prentice-Hall, Inc., Englewood Cliffs, New Jersey.

Wilson, B.W. (1965): Numerical prediction of ocean waves in the North Atlantic for December, 1959. Deut. Hydrogr. Z., Band 18, Heft 3, pp. 114-130.

Appendix I. Coded symbols, observation time differences, wind speed, significant height, and location of the data used in Figure 3.

Data Source	Identification	Symbol	Δt (hours)	Wind speed (knots)	$\overline{H}_{\frac{1}{3}}$ (ft)	Location
British weather ships (Moskowitz, Pierson, and Mehr, 1962, 1963, 1965)	JHC 38-39	⊕	6	45-42	27.4-37.3	I
	JHC 73-74	x	3	43-43	23.8-33.3	I
	DL 37-38	⊙	6	33-32	14.3-17.9	I
	JH 10-11	▽	6	37-37	15.2-2.10	K
	DL 55-56	I	6	38-40	24.9-28.3	I
	JHA 9-10	o	3	60-61	26.1-32.9	J
	DL 77-78	△	3	42-43	16.6-21.7	A
Argas Island Tower (Pickett, 1962); DeLeonibus (1962)	25 Nov. 1961	⋋	12Z-15Z	28-30	10.8-12.3	
Towed raft Snyder and Cox (1966)		+				
Airborne altimeter (Barnett and Wilkerson, 1966)		•				

Appendix II. Air-sea temperature difference (°C)

British weather ships (Moskowitz, Pierson and Mehr)

JHC 38-39	Apr. 8, 1955	(-0.5) ~ (-0.4)
JHC 73-74	May 11, 1956	(-1.5) ~ (-0.2)
DL 37-38	Oct. 28, 1958	(-0.9) ~ (-3.9)
JH 10-11	Mar. 29, 1959	(-1.1) ~ (-2.1)
DL 55-56	Nov. 9, 1959	(-5.8) ~ (-7.0)
JHA 9-10	Dec. 17, 1959	(-3.8) ~ (-3.1)
DL 77-78	Jan. 30, 1960	(-0.6) ~ (-1.7)

Airborne altimeter (Barnett and Wilkerson, 1966)

(-6°) ~ (-10°)

Towed raft (Snyder and Cox, 1966)

Almost neutral condition.

Largest difference (-0.7)

Appendix III. Wind velocity for the test run period, December 1959.

Date	time (GMT)	Weather ship Speed (kts)	Weather ship Dir. (°)	Grid point 72 Speed (kts)	Grid point 72 Dir. (°)	Grid point 73 Speed (kts)	Grid point 73 Dir. (°)
Dec. 16	00	10	340	25.3	270	25.7	278
	06	04	280	21.1	215	22.1	246
	12	23	170	28.3	209	28.0	194
	18	32	250	37.9	243	36.9	234
Dec. 17	00	60	250	34.7	270	35.8	257
	06	48	280	41.9	268	44.8	252
	12	48	290	48.0	286	46.8	276
	18	48	290	48.7	293	50.4	283
Dec. 18	00	40	320	21.8	297	33.6	295
	06	20	280	16.3	277	30.7	288
	12	26	180	31.2	160	18.8	171
	18	26	210	34.2	171	32.5	165
Dec. 19	00	30	220	22.5	216	23.1	207
	06	18	250	27.6	221	28.8	215
	12	28	240	26.0	240	30.0	232
	18	17	250	30.7	233	31.6	224
Dec. 20	00	28	270	24.2	264	27.7	252
	06	36	280	24.3	260	29.7	253
	12	28	260	29.9	255	31.0	259
	18	16	250	27.1	262	30.7	251
Dec. 21	00	28	270	26.8	272	28.3	258
	06	27	310	16.5	269	21.8	259
	12	07	270	7.9	239	15.7	264
	18	23	170	18.2	178	14.0	187

Date	time (GMT)	Weather ship Speed (kts)	Weather ship Dir. (°)	Grid point 72 Speed (kts)	Grid point 72 Dir. (°)	Grid point 73 Speed (kts)	Grid point 73 Dir. (°)
Dec. 22	00	35	220	32.8	220	27.9	201
	06	40	230	47.2	237	43.1	231
	12	40	250	37.8	251	37.4	230
	18	50	270	38.2	244	39.2	224
Dec. 23	00	55	270	45.5	269	45.9	257
	06	43	280	45.2	257	44.1	247
	12	45	290	41.7	287	40.4	269
	18 (21Z)	40	300	41.0	292	41.0	281
Dec. 24	00			34.8	293	38.6	293
	06	32	290	22.9	285	32.7	287
	12	20	270	7.5	249	20.0	275
	18	18	160	12.1	144	6.3	216
Dec. 25	00	43	130	24.7	129	32.8	128
	06	21	160	14.3	166	24.3	159
	12	19	230	9.8	244	17.0	206
	18	25	210	17.2	264	26.1	224
Dec. 26	00	37	250	22.2	273	28.9	241
	06	23	270	26.8	287	31.4	259
	12	22	290	21.1	293	24.9	259
	18 21Z	18	360	24.5	295	27.4	271
Dec. 27	00						
	03	23	360	19.3	295	22.6	274
	06						
	09	28	320	23.3	298	26.4	293
	12						
	15	25	330	26.6	299	29.8	303
	18						
	21	23	300	20.7	289	27.2	285